

**Faculty of Engineering & Technology
Electrical & Computer Engineering Department**

CONTROL AND POWER ELECTRONICS LAB (ENEE4105)

Report 1

“Three-Phase Controlled Rectifiers”

Prepared by:

Eman Asfour 1200206

Partners:

Sadeel Ali 1200487

Abdullah Qashoo 1190685

Instructor: Dr. Hakam

Shehadeh

Assistant: Eng.Rafah Rahhal

Section: 2

Date: 21/03/2024

Place: Aggad345

Table of Contents

1.	Abstract	3
2.	Method used	3
3.	<i>Theory</i>	1
■	Three-phase Controlled Rectifier.....	1
1)	Three-Phase Half-Wave Controlled Rectifier	2
2)	Three-Phase Semi-Converter.....	4
3)	Three-Phase Full-Converter:	6
■	Applications of Controlled Rectifiers: Powering Diverse Technologies.....	7
4.	Procedure, Data, and Calculations.....	9
A.	Three-Phase Half-wave Converter.....	9
a.	Three-Phase Half-wave Converter with Resistive Load	9
b.	Three-Phase Half-wave Converter with Resistive-inductive Load	19
B.	Three-Phase Semi-Converter.....	24
a.	Three-Phase Semi-Converter with Resistive Load	24
a)	Three-Phase Semi-Converter with Resistive-Inductive Load.....	32
A.	Three-Phase Full-Converter	37
a)	Three-Phase full-Converter with Resistive Load.....	37
b)	Three-phase full-Converter with resistive-Inductive Load	43
5.	Discussion and Results.....	49
A.	Three-Phase Half-wave Converter.....	49
B.	Three-Phase Semi-Converter	49
C.	Three-Phase Full-Converter	50
6.	Conclusion.....	52
7.	References.....	53

1. Abstract

The objective of this experimental study is to explore and analyze various configurations of Three-Phase Controlled Rectifiers under diverse load conditions. By setting up different topologies, the experiment aims to measure and interpret crucial parameters associated with these rectifiers. Furthermore, it seeks to deepen understanding by elucidating the operational principles and deriving control characteristics of different types of Three-Phase Controlled Rectifiers. Through meticulous analysis and practical exploration, this study endeavors to furnish a comprehensive insight into the functioning and applications of Three-Phase Controlled Rectifiers in the realm of power electronics, thereby contributing to the advancement of this field.

2. Method used

1 Load, Power Electronics	735 09
1 Phase Commutated Converter	735 012
1 Converter Controller Unit	735 122
1 Phase Control Noise Filter 3X4.5A	735 190
1 Transformer 45/90, 3 N	726 80
1 Sensor-CASSY 2 – Starter	524 013S
1 Mask (Bridge Topology)	735 012 – 03 M3C
1 Mask (Bridge topology)	735 012 – 08 B6C
1 Mask (Bridge topology)	735 012 – 09 B6HA, B6HK
1 Set of 10 safety bridging plugs, black	500 59
1 Set of 10 safety bridging plugs with a tap, black	500 591
2 Safety Connection Lead 100 cm yellow/green	500 640
Safety Connection Lead 100 cm, red	500 641

Table 1: The method used in the experiment

Table of Figures

Figure 1: Three Phase Controlled rectifiers with purely resistive load [3].....	2
Figure 2: The Output of three phase half wave converter [1]	3
Figure 3: Three-Phase Semi-Converter [5]	4
Figure 4: The output of three phase semi-converter [2]	5
Figure 5: Three-phase full-converter [7]	6
Figure 6: The Output of three-phase full-converter [2].....	6
Figure 7: The RMS Input voltage and Input current	9
Figure 8: The Averages values of Input voltage and Input Current	10
Figure 9: The SCR voltage and the Input current.....	11
Figure 10: The Average voltage output and current output when delay angle =45	12
Figure 11: The RMS output voltage and output current when delay angle =45	12
Figure 12: The Frequency of the output of delay angle =45	13
Figure 13: The voltage input and current input when delay angle =90.....	14
Figure 14: The voltage on SCR with input current	15
Figure 15: The RMS output voltage and output current when delay angle =90	15
Figure 16: The frequency of the output voltage when delay angle =90	16
Figure 17: Normalized Measured and Calculated Output Voltage	18
Figure 18: Configuration of Three-Phase Half-Wave Converter supplying a Resistive - Inductive load of 33.3Ω & $50mH$	20
Figure 19: The RMS input voltage and the input current when $\alpha =45$ in SemiConverter with RL	20
Figure 20: The relationship between the RMS (Root Mean Square) and average values of a waveform.....	20
Figure 21: The mean of the input voltage and current for delay angle =45	21
Figure 22: The SCR voltage (UV) and the input current (is) when $\alpha =45$ in Half-Wave Converter with RL.....	21
Figure 23: The output voltage and current in the average value of dealy angle = 45	22
Figure 24: The Output voltage and current in RMS value in dealy angle=45.....	22
Figure 25:The average output voltage and current of dealy angle =90	23
Figure 26: The RMS output voltage of delay angle 90	23
Figure 27: Configuration of Three-Phase Semi-Converter supplying a purely resistive load of 300Ω	25
Figure 28: The input voltage (us01) and the input current (is) when $\alpha =45$ in Semi-Converter with R.....	25
Figure 29: The average input voltage (us01) and the input current (is) when $\alpha =45$ in Semi-Converter with R	26
Figure 30: The SCR1 (valve) voltage and SCR1 (valve) current when $\alpha =45$ in Semi-Converter with R	26
Figure 31 :The average output voltage and the output current when $\alpha =45$ in Semi-Converter with R.....	27
Figure 32:The RMS of the output voltage and the output current when $\alpha =45$ in Semi-Converter with R.....	28
Figure 33:The frequency of the output voltage	28
Figure 34: The RMS of the output voltage and the output current when $\alpha =90$ in Semi-Converter with R.....	29
Figure 35: The average of the output voltage and the output current when $\alpha =90$ in Semi-Converter with R.....	30
Figure 36: The frequency of the output voltage	30
Figure 37: The normalized measured and calculated output voltage as a function of delay angle for a semi-converter with resistive load.....	32
Figure 38:Configuration of Three-Phase Semi-Converter supplying an RL load of 300Ω and $50mH$	33
Figure 39:The RMS Input voltage and current of the there phase semi-converter with dealy angle =45	33
Figure 40: The Average Input voltage and current of the there phase semi-converter with dealy angle =45	33
Figure 41: The Average voltage and current of Three-Phase Semi-Converter with Resistive-Inductive Load of dealy angle =45	34
Figure 42: The average output voltage and the output current when $\alpha =45$ in Semi-Converter with RL	35
Figure 43:The RMS output voltage and the output current when $\alpha =45$ in Semi-Converter with RL	35
Figure 44:The RMS of the output voltage and current with RL and delay angle =90	36
Figure 45: The Average output voltage and current with RL and delay angle =90	36
Figure 46: Configuration of Three-Phase Full-Converter supplying a purely resistive load of 300Ω	38
Figure 47: The Voltage and current of the SCR with dealy angle =45 for full-converter with R	39
Figure 48: The RMS output voltage of a three-phase full-converter with R of dealy angle =45	39

Figure 49: The average output of a three-phase full-converter with R of dealy angle =45.....	40
Figure 50: The measured to calculate the frequency of three-phase full-wave converters with dealy angle =45.....	40
Figure 51: The normalized measured and calculated output voltage as a function of delay angle =45 for Full-phase converter.....	42
Figure 52: The RMS of the output voltage of a three-phase full-converter with dealy angle =90.....	43
Figure 53: Configuration of Three-Phase Full-Converter supplying an RL load of 300Ω and 50mH	43
Figure 54: The RMS input voltage and current input of a three-phase full converter with dealy angle=45 with RL.	44
Figure 55: The voltage and current on the SCR of a three-phase full converter with dealy angle =45	45
Figure 56: The average Voltage of three phase full conveter with RL & dealy angle =45	45
Figure 57: The RMS Voltage of a phase full converter with RL & dealy angle =45.....	46
Figure 58: The RMS Output voltage of three-phase converter with RL & dealy angle =90	46
Figure 59: The average output of a three-phase converter with RL & dealy angle =90	47

Table of tables

Table 1:The effect of the delay angle on the average value of output voltage and current of a Three-Phase Half-Wave.....	18
Table 2: The Values of The output of Three phase half wave controlled rectifier with RL and dealy angle =45	22
Table 3: The output voltage of dealy angle =90.....	23
Table 4: The input voltage and current of semi-converter R of dealy angle =45.....	26
Table 5: The Output voltage of the Semi-converter of dealy angle=45 with R	28
Table 6: The output of the semi-converter with delay angle =90.....	30
Table 7: The Output of Semi-converter with RL and delay angle =45	35
Table 8: The Output of Three-phase semi-converter of dealy angle =90 RL.....	36
Table 9: The Output voltage of a three-phase full converter with delay angle =45	40
Table 10: The theoretical value of three-phase full-converter	41
Table 11: The normalized measured and calculated output voltage of delay angle=45 for Full-phase converter	41
Table 12: The Output of a three-phase full converter with RL & dealy angle =90.....	48

Table of Equations

Equation 1: The average output voltage of a Three-Phase Half-Wave Converter for resistive load [1].....	3
Equation 2: The root-mean-square of a Three-Phase Half-Wave Converter for a resistive load.....	3
Equation 3: The average output voltage of a Three-Phase Half-Wave Converter for a highly inductive load	3
Equation 4: The rms value of the output voltage of a Three-Phase Half-Wave Converter for a highly inductive load	3
Equation 5: The average output voltage of a Three-Phase Semi-Converter	5
Equation 6: The Root-mean-square of the output voltage for $\alpha > \pi/3$	5
Equation 7: Equation 6: The Root-mean-square of the output voltage for $\alpha \leq \pi/3$	5
Equation 8: The average output voltage of a Three-Phase Full-converter	6
Equation 9: The rms value of the output voltage of a Three-Phase Full- Converter for a highly inductive load.....	6
Equation 10: Equation 8: The average output voltage of a Three-Phase Full-converter in the resistive load.....	7
Equation 11: The Frequency Formula	13
Equation 12: The difference between the two time periods	13
Equation 13: The Form Factor	13
Equation 14: The Ripple Factor	14
Equation 15: The Transformer Unitization Factor	14
Equation 16: The Frequency Formaula	16
Equation 17: The difference between the two time periods	16
Equation 18: The Form Factor	17
Equation 19: The Ripple Factor	17
Equation 20: The Transformer Unitization Factor	17
Equation 21: The Form Factor	22
Equation 22: The Ripple Factor	23
Equation 23: The Transformer Unitization Factor	23
Equation 24: The Ripple Factor	24
Equation 25: The Transformer Unitization Factor	24
Equation 26: The Frequency Formula	28
Equation 27: The difference between the two time periods	28
Equation 28: The Form Factor	29
Equation 29: The Ripple Factor	29
Equation 30: The Transformer Unitization Factor	29
Equation 31: The Form Factor	29
Equation 32: The Ripple Factor	29
Equation 33: The Transformer Unitization Factor	29
Equation 34: The Form Factor	30
Equation 35: The Ripple Factor	30
Equation 36: The Transformer Unitization Factor	30
Equation 37: The Frequency Formula	30
Equation 38: The difference between the two time periods	30
Equation 39:the peak-to-peak ripple	31
Equation 40: The Frequency Formula	40
Equation 41: The difference between the two time periods	40
Equation 42: The Form Factor	41
Equation 43: The Ripple Factor	41
Equation 44: The Transformer Unitization Factor	41
Equation 45: The Form Factor	41
Equation 46: The Ripple Factor	41

3. Theory

▪ Three-phase Controlled Rectifier

Controlled Rectifiers represent essential power electronic circuits engineered for the conversion of AC voltage (or current) into controllable DC voltage (or current). These rectifiers yield an output comprising a regulated DC component alongside additional unwanted AC components termed harmonics. The functionality of controlled rectifiers encompasses the modulation of AC inputs into precise DC outputs, catering to a myriad of applications across industries ranging from renewable energy systems to motor control. By harnessing advanced control techniques, these rectifiers play a pivotal role in enhancing power efficiency while mitigating the adverse effects of harmonic distortion, thereby underscoring their significance in modern power electronics. [1]

1) Three-Phase Half-Wave Controlled Rectifier

The Three-Phase Half-Wave Controlled Rectifier is a fundamental power electronic circuit used to convert three-phase AC voltage into a controllable DC output. In this configuration, each phase of the AC supply is connected to a thyristor, allowing for individual control of the rectification process. During each half-cycle of the AC input, the thyristors are triggered to conduct, allowing current flow through the load. By controlling the firing angle of the thyristors, the output voltage and power delivered to the load can be regulated. However, this rectifier configuration produces significant harmonic distortion due to its simplistic design, limiting its use in applications requiring high-quality DC output. Despite its drawbacks, the Three-Phase Half-Wave Controlled Rectifier remains a crucial building block in understanding more complex rectifier topologies and power conversion techniques.

When a three-phase controlled rectifier is connected to a purely resistive load, the current drawn from the rectifier aligns perfectly with the voltage waveform. This results in a power factor of 1, indicating an efficient use of electrical power without any phase shift between voltage and current. Such configurations are commonly found in industrial heating applications where the load primarily involves resistive elements, such as in electric furnaces or heating elements. Here, the rectifier efficiently converts AC power to DC, allowing precise control over the heat output.

The output voltage and current of a three-phase controlled rectifier with a resistive load have only one polarity, indicating that the converter operates within a single quadrant. In this configuration, both voltage and current are positive, leading to power delivery from the rectifier to the load. This characteristic makes it suitable for applications where power flow is unidirectional, such as in heating systems, DC power supplies, or battery charging. The rectifier efficiently converts AC input to DC output, providing a stable and controllable power source for resistive loads. Even with a purely resistive load, if the firing angle α is less than $\pi/6$, the output voltage remains continuous and sustains the same average value as it would with a highly inductive load. This observation also extends to the root mean square (RMS) value of the output voltage. [2]

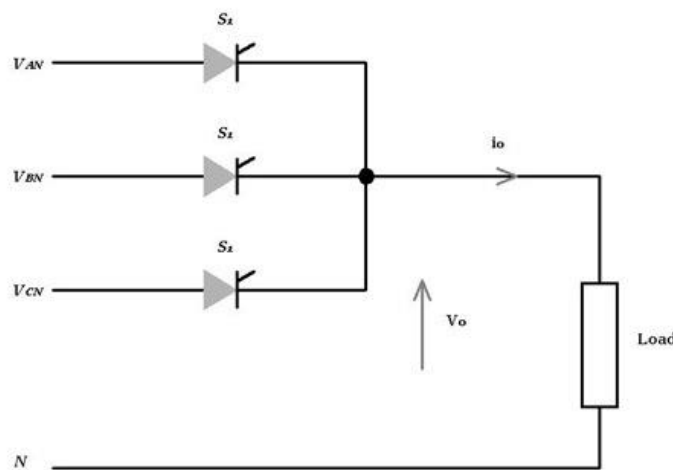


Figure 1: Three Phase Controlled rectifiers with purely resistive load [3]

$$V_{dc} = \frac{3V_m}{2\pi} (1 + \cos(\frac{\pi}{6} + \alpha)) ; \quad \frac{\pi}{6} < \alpha < \frac{5\pi}{6}$$

Equation 1: The average output voltage of a Three-Phase Half-Wave Converter for resistive load [1]

$$V_{rms} = \sqrt{3} V_m \sqrt{\left(\frac{5}{24} - \frac{\alpha}{4\pi} + \frac{1}{8\pi} \sin\left(\frac{\pi}{3} + 2\alpha\right) \right)} \quad \frac{\pi}{6} < \alpha < \frac{5\pi}{6}$$

Equation 2: The root-mean-square of a Three-Phase Half-Wave Converter for a resistive load

On the other hand, when connected to a purely inductive or highly inductive load, the current waveform lags behind the voltage waveform due to the inductive nature of the load. This leads to a phase shift between voltage and current, resulting in a lagging power factor. In such cases, the rectifier needs to handle reactive power in addition to real power, which may require additional components for power factor correction. Applications involving inductive loads include motor drives, transformers, and certain types of lighting systems. In these applications, the rectifier plays a crucial role in converting AC power while managing the reactive components effectively to ensure smooth operation and efficient energy usage.

$$V_{dc} = \frac{3\sqrt{3} V_m}{2\pi} \cos(\alpha) ; \quad 0 < \alpha < \pi$$

Equation 3: The average output voltage of a Three-Phase Half-Wave Converter for a highly inductive load

$$V_{rms} = \sqrt{3} V_m \sqrt{\left(\frac{1}{6} + \frac{\sqrt{3}}{8\pi} \cos(2\alpha) \right)} ; \quad 0 < \alpha < \pi$$

Equation 4: The rms value of the output voltage of a Three-Phase Half-Wave Converter for a highly inductive load

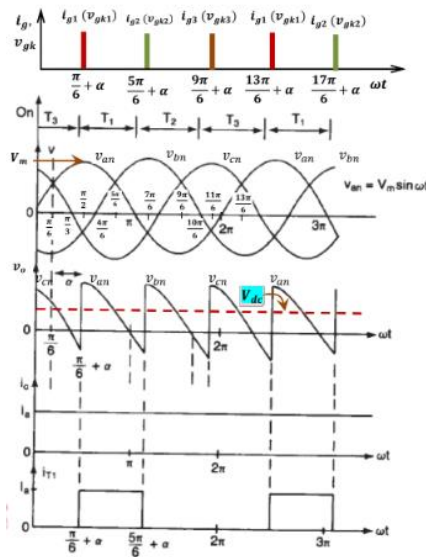


Figure 2: The Output of three phase half wave converter [1]

2) Three-Phase Semi-Converter

Three-phase semi-converters are commonly employed in industrial power applications up to approximately 120 kW, particularly when single-quadrant operation is necessary. As the trigger angle α increases, the power factor of the three-phase semi-converter decreases. Nonetheless, it still maintains a better power factor compared to a three-phase half-wave converter. In a typical configuration with a highly inductive load, the operation of the semi-converter involves the forward biasing of thyristors and diodes based on the phase supply voltages. Specifically, thyristors are triggered when their corresponding phase supply voltage is positive and greater than the others, while diodes conduct when their respective phase supply voltage is more negative than the others. The waveform diagrams illustrate the behavior of the input supply voltages, output voltage, thyristor and diode currents, current through the freewheeling diode, and the overall supply current. The frequency of the output supply waveform is triple the input AC supply frequency. The trigger angle α can be adjusted from 0° to 180° to regulate the output of the semi-converter. [4]

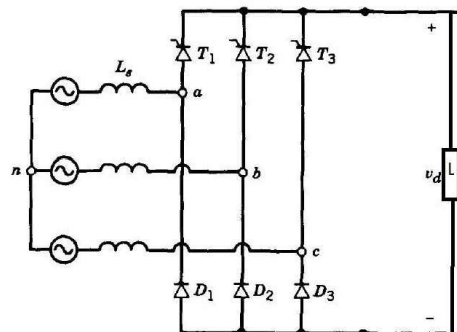


Figure 3: Three-Phase Semi-Converter [5]

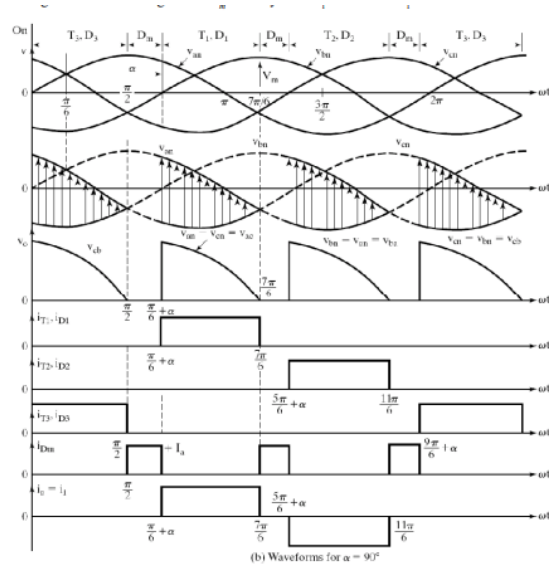


Figure 4: The output of three phase semi-converter [2]

$$V_{dc} = \frac{3\sqrt{3} V_m}{2\pi} (1 + \cos(\alpha)) ; \quad 0 < \alpha < \pi$$

Equation 5: The average output voltage of a Three-Phase Semi-Converter

$$V_{rms} = \sqrt{3} V_m \sqrt{\left(\frac{3}{4\pi} (\pi - \alpha + \frac{\sin 2\alpha}{2}) \right)} ; \quad \frac{\pi}{3} \leq \alpha \leq \pi$$

Equation 6: The Root-mean-square of the output voltage for $\alpha > \frac{\pi}{3}$

For $\alpha > \frac{\pi}{3}$ and discontinuous output voltage

$$V_{rms} = \sqrt{3} V_m \sqrt{\left(\frac{3}{4\pi} \left(\frac{2\pi}{3} + \sqrt{3}(\cos \alpha)^2 \right) \right)}$$

Equation 7: Equation 6: The Root-mean-square of the output voltage for $\alpha \leq \frac{\pi}{3}$

For $\alpha \leq \frac{\pi}{3}$, and continuous output voltage

3) Three-Phase Full-Converter:

The Three-Phase Full Converter is a fully controlled bridge rectifier utilizing six thyristors arranged in a full-wave bridge configuration. Each thyristor serves as a controlled switch, triggered at appropriate times through suitable gate signals. Widely applied in industrial power settings up to 120 kW, particularly for two-quadrant operations, this converter is also referred to as a three-phase full-wave bridge or a six-pulse converter. With a highly inductive load, thyristors are triggered at intervals of $\pi/3$ radians (equivalent to 60°). The output ripple voltage frequency is 6 times the input AC frequency, and the filtering requirement is less demanding compared to three-phase semi and half-wave converters. [6]

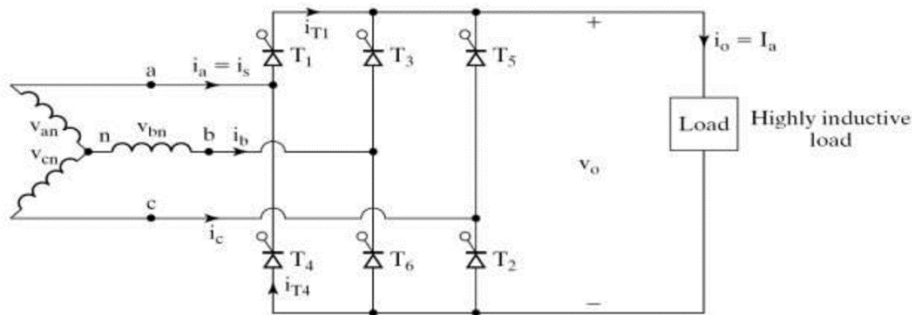


Figure 5: Three-phase full-converter [7]

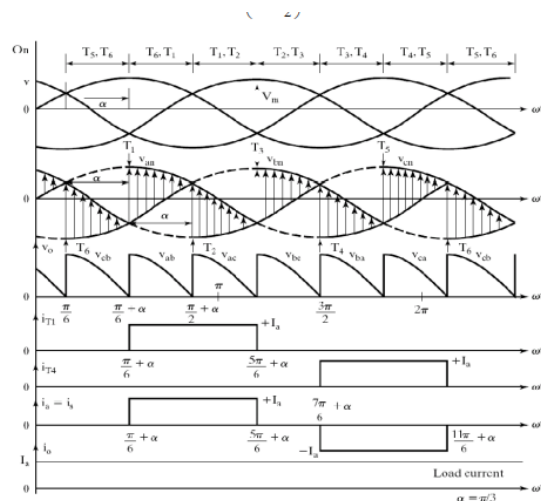


Figure 6: The Output of three-phase full-converter [2]

$$V_{dc} = \frac{3\sqrt{3}}{\pi} V_m (1 + \cos(\alpha)) ; \quad 0 \leq \alpha \leq \pi$$

Equation 8: The average output voltage of a Three-Phase Full-converter

$$V_{rms} = \sqrt{3} V_m \sqrt{\left(\frac{1}{2} + \frac{3\sqrt{3}}{4\pi} \cos 2\alpha\right)}$$

Equation 9: The rms value of the output voltage of a Three-Phase Full- Converter for a highly inductive load

When α is less than $\frac{\pi}{3}$, the output voltage remains continuous without any negative instantaneous values, regardless of whether the load is resistive or highly inductive. Consequently, for $\alpha < \frac{\pi}{3}$, the average output voltage remains consistent regardless of the type of load, whether resistive or highly inductive. In the case of a highly inductive load and $\alpha > \frac{\pi}{3}$, the instantaneous output voltage exhibits negative portions. However, when dealing with a resistive load and $\alpha > \frac{\pi}{3}$, the instantaneous output voltage cannot be negative due to the inability of the output current to be negative.

$$V_{dc} = \frac{3\sqrt{3} V_m}{\pi} \left(1 + \cos\left(\alpha + \frac{\pi}{3}\right)\right); \quad \frac{\pi}{3} \leq \alpha \leq \frac{4\pi}{6}$$

Equation 10: Equation 8: The average output voltage of a Three-Phase Full-converter in the resistive load

▪ Applications of Controlled Rectifiers: Powering Diverse Technologies

Controllable rectifiers, including half-wave, full-wave, and semi-three phase configurations, find extensive application in various aspects of our daily lives. These rectifiers play crucial roles in converting alternating current (AC) into direct current (DC) with controllable output voltages. Half-wave rectifiers are commonly used in small power supplies, battery chargers, and dimmer switches, where moderate power requirements and simple control suffice. Full-wave rectifiers, on the other hand, are employed in a wide range of applications such as motor drives, battery charging systems, and uninterruptible power supplies (UPS), due to their higher efficiency and smoother output. Semi-three phase rectifiers are particularly useful in medium to high-power applications like industrial drives, traction systems, and renewable energy systems, where the demand for controlled and efficient power conversion across three phases is essential. These rectifier configurations enable precise control over the output voltage, making them indispensable in modern electronics, transportation, industrial automation, and renewable energy sectors, contributing significantly to enhancing energy efficiency and performance in various aspects of our daily lives. [8]

4. Procedure, Data, and Calculations

A. Three-Phase Half-wave Converter

a. Three-Phase Half-wave Converter with Resistive Load

i. Three-Phase Half-wave Converter with Resistive Load when delay angle =45

The transformer secondary was connected to produce a phase-to-neutral voltage of 45V. Resistors of 33.3 ohms were connected in parallel with 100 ohms. The mask Bridge topology 735012-03MC was utilized. The converter control unit (735 122) was adjusted to set the delay angle to 45 degrees. Subsequently, the transformer supply voltage (Cat. No 726 80) was turned on. Following this, the input voltage and input current were plotted, and their RMS and average values were measured. The probe of Cassy lab was connected to measure and plot the SCR voltage, keeping the input current constant. The transformer supply voltage was turned off, and the probe was then connected to measure and plot the output voltage and output current. Upon turning on the transformer, the output voltage and current were plotted, and the peak-to-peak ripple at the output voltage was measured, along with the average and RMS values of the output current and voltage. Following this, the transformer was turned off to adjust the converter control unit to set the delay angle to 90 degrees. The transformer supply voltage was turned off, and the probe was connected to measure and plot the output voltage and output current. Upon turning on the transformer, the output voltage and current were plotted, and the peak-to-peak ripple at the output voltage was measured, along with the average and RMS values of the output current and voltage. The delay angle was then adjusted according to Table 1, ranging from 0 to 150, and the average output current and voltage were measured.

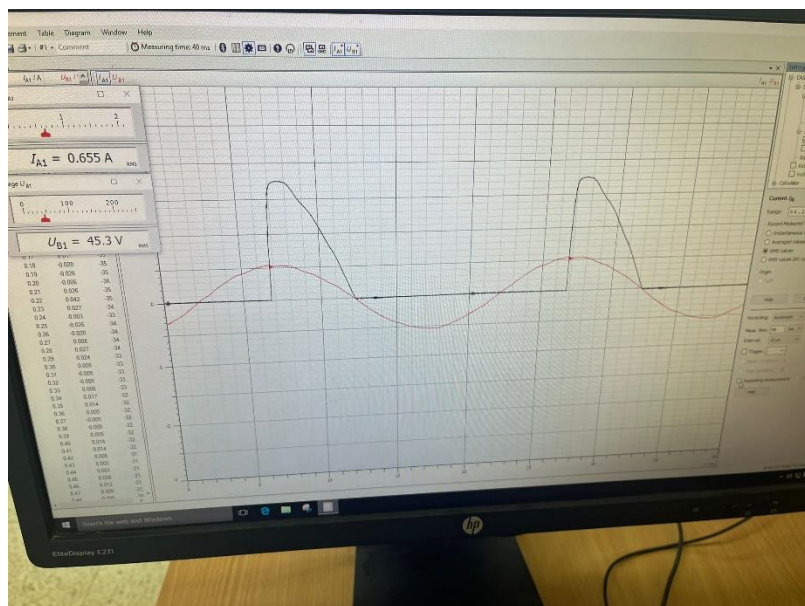


Figure 7: The RMS Input voltage and Input current

- The Input current
- The Input voltage

In a three-phase half-wave controlled rectifier circuit, each phase of the three-phase AC input is linked to a thyristor. These thyristors serve as switches that activate and deactivate at specific junctures in the AC cycle, regulated by a firing circuit. The firing angle dictates the timing of thyristor activation during the positive half cycle of the AC voltage, thereby influencing the average DC output voltage supplied to the load. To smooth out the pulsating DC output from the rectifier, a filter is typically incorporated before the thyristor. Commonly, this filter consists of a capacitor. On the input side of the filter, the current waveform mirrors that of the output side, albeit in an inverted fashion.

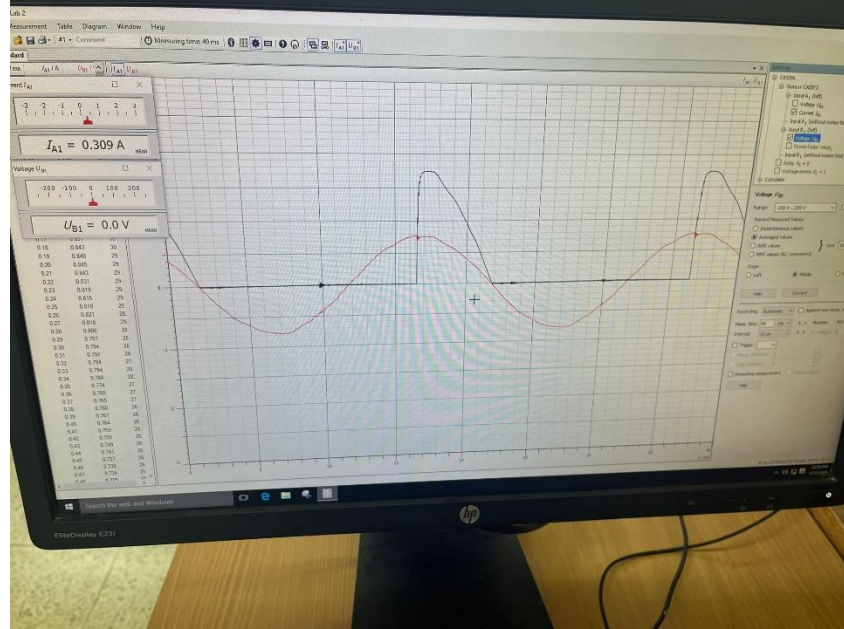


Figure 8: The Averages values of Input voltage and Input Current

The distinction between the average and RMS values of current and voltage in a three-phase half-wave controlled rectifier circuit is significant and reflects the unique traits of this rectification method. In such setups, average values indicate the mean magnitude of current and voltage over a complete cycle, while RMS (Root Mean Square) values denote the effective or equivalent value of the alternating current or voltage. Regarding current, the average value (0.309 A) typically falls below the RMS value (0.655 A). This variance stems from the average value solely considering the current's magnitude during its flow time, predominantly occurring in the positive half-cycle of the AC input waveform. Conversely, the RMS value accounts for the squared current values throughout the cycle, encompassing both positive and negative half-cycles, yielding a higher outcome. Likewise, with voltage, the average value (0.0 V) reflects the fact that in a half-wave rectifier, voltage application occurs solely during a segment of the cycle, specifically the positive half-cycle, resulting in an average of zero across the complete cycle. However, the RMS value (45.3 V) integrates the effective voltage across the load, encompassing both positive and negative waveform sections, resulting in a nonzero outcome. In essence, the disparity between average and RMS values in a three-phase half-wave controlled rectifier circuit emphasizes the importance of grasping both the instantaneous and effective characteristics of current and voltage waveforms in such setups.

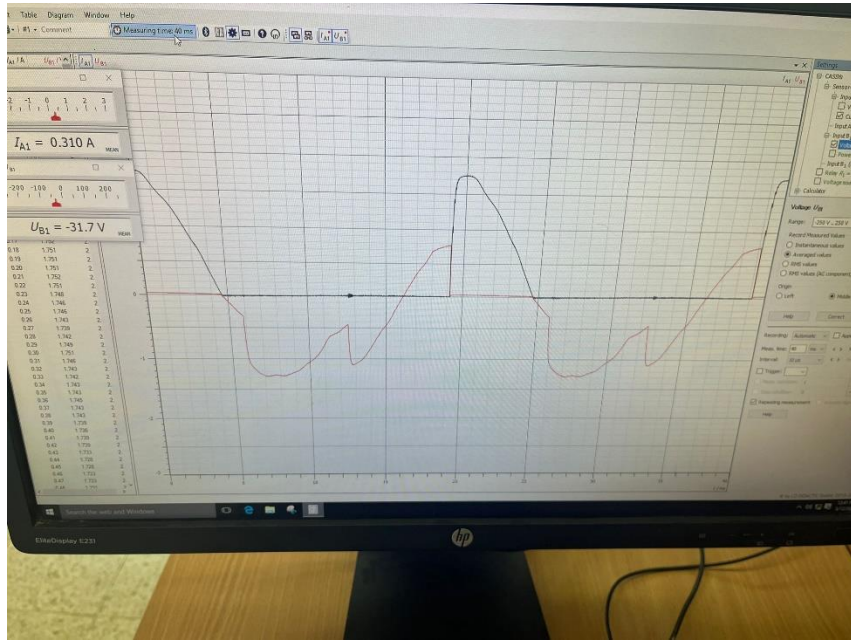


Figure 9: The SCR voltage and the Input current

SCR Voltage (Red Trace): The SCR voltage waveform typically mirrors the positive half cycles of the AC input voltage waveform, albeit with some delay due to the firing angle of the SCR. During the negative half cycles of the AC voltage, the SCR becomes reverse biased, resulting in the voltage across it approaching zero. **Input Current (Black Trace):** The input current waveform manifests as a series of pulses corresponding to the positive half cycles of the AC voltage. The width of these pulses is contingent upon the firing angle of the SCR. A smaller firing angle results in wider pulses and a higher average DC output voltage, whereas a larger firing angle yields narrower pulses and a lower average DC output voltage. For a firing angle of 45 degrees, the input current measures 0.310, while the SCR voltage is -31.7. It's important to note that the figures presented are in average values .SCR voltage, unlike AC waveforms, does not possess an RMS (Root Mean Square) value in the conventional sense. Instead, it is characterized by its on-state voltage drop and off-state voltage blocking capability. When the SCR conducts (forward biased), it incurs a relatively constant voltage drop, often referred to as the "forward voltage drop" or "on-state voltage." This voltage drop remains fixed for a specific SCR and operating conditions and does not adhere to an RMS value akin to AC waveforms. Conversely, when the SCR is turned off (reverse biased), the voltage across it can spike considerably. In this scenario, it is crucial to consider the peak and average values rather than an RMS value. Thus, while SCR voltage lacks an RMS value, its attributes are typically articulated in terms of its on-state voltage drop and off-state peak or average voltage.

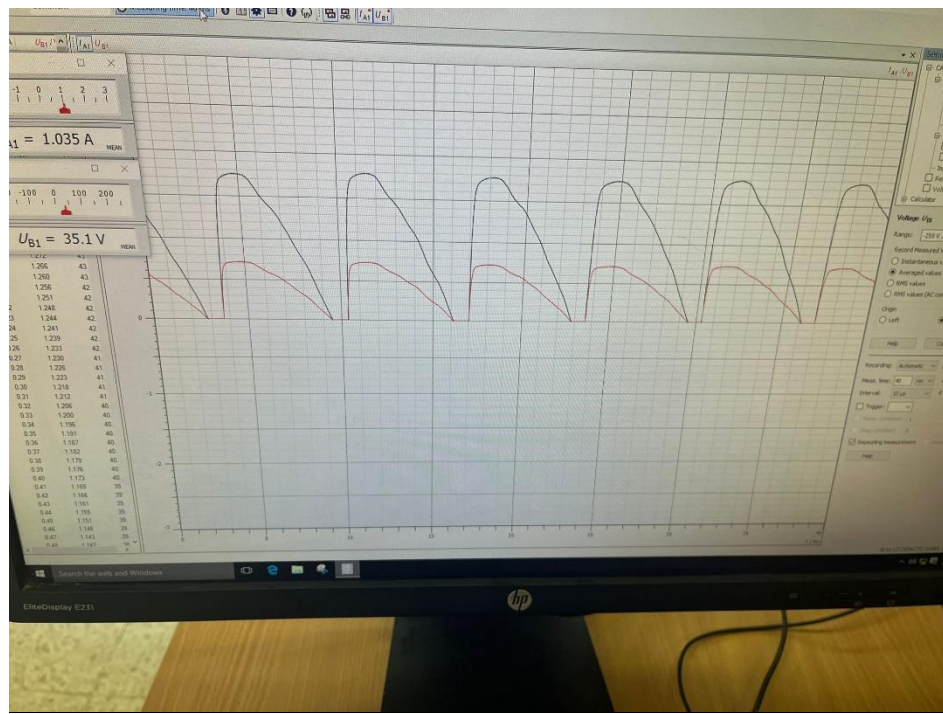


Figure 10: The Average voltage output and current output when delay angle =45

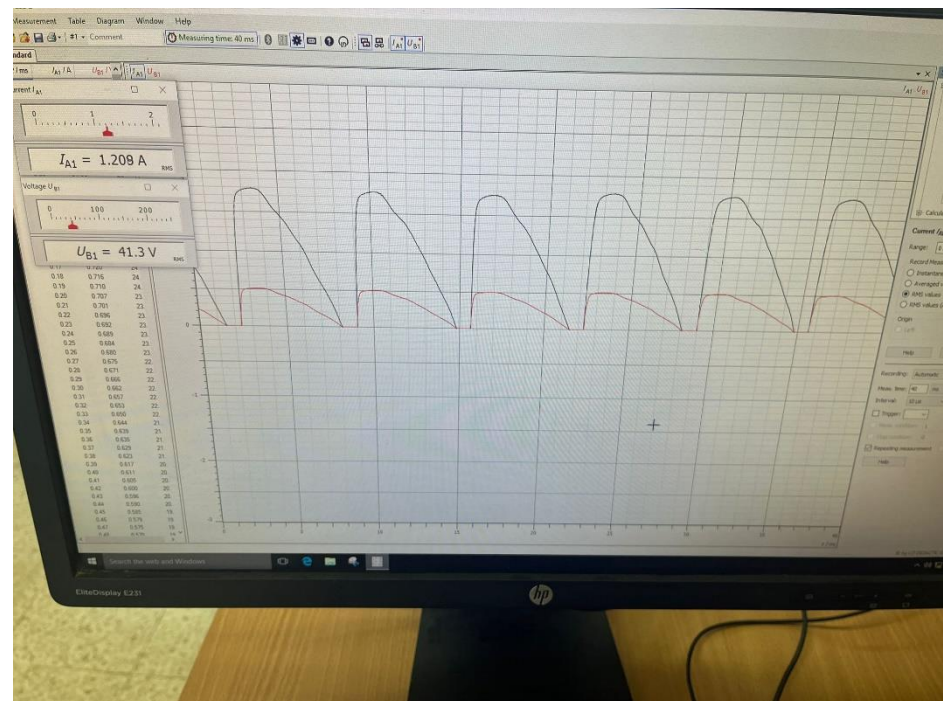


Figure 11: The RMS output voltage and output current when delay angle =45

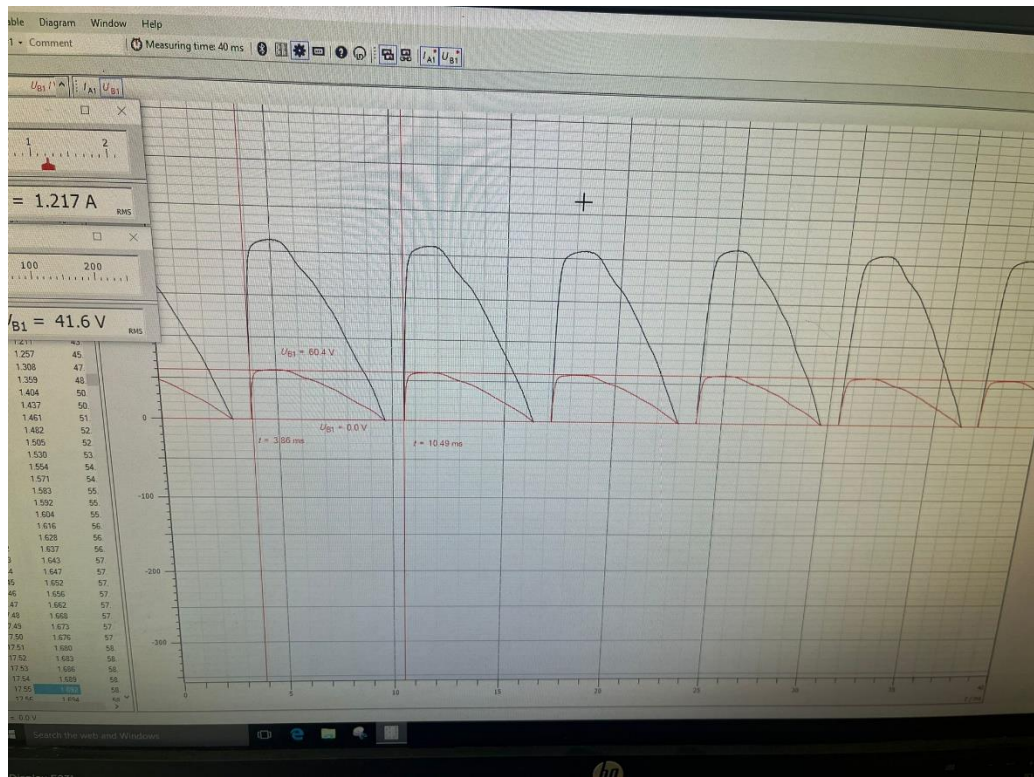


Figure 12: The Frequency of the output of delay angle =45

$$f = \frac{1}{T} = 150.82 \text{ Hz}$$

Equation 11: The Frequency Formula

$$T = T_2 - T_1 = 6.63\text{ms}$$

Equation 12: The difference between the two time periods

In analyzing the figures for a three-phase half-wave controlled rectifier with a resistive load of 300 ohms, it's evident that the RMS output current and voltage measure at 1.209 A and 41.3 V respectively, while the average values are 1.035 A and 35.1 V. Notably, fluctuations in voltage and current occur over time due to the rectification process. In instances where voltage and current approaches zero, they later exhibit values like Mean V=35.1 V and I=1.035 A. These fluctuations are a consequence of each phase incorporating one thyristor, leading to pulsating current and voltage outputs during forward conduction. However, despite these variations, in purely resistive loads, the output current shares the same wave shape as the output voltage, ensuring a consistent and stable power delivery to the load.

$$FF = \frac{V_{RMS}}{V_{DC}}$$

Equation 13: The Form Factor

$$FF = \frac{V_{RMS}}{V_{DC}} = \frac{41.3}{35.1} = 1.18$$

$$RF = \sqrt{(FF^2 - 1)} = 0.620$$

Equation 14: The Ripple Factor

$$TUF = \frac{P_{DC}}{3 * V_s * I_s} = \frac{1.035 * 35.1}{0.655 * 45.3} = 1.24$$

Equation 15: The Transformer Utilization Factor

$V_m = 45$ V phase to neutral

$\alpha = 45^\circ$

$$V_{dc} = \frac{3V_m}{2\pi} \left(1 + \cos\left(\frac{\pi}{6} + \alpha\right) \right) = 34.5 \text{ V}$$

$$V_{rms} = \sqrt{3} V_m \sqrt{\left(\frac{5}{24} - \frac{\alpha}{4\pi} + \frac{1}{8\pi} \sin\left(\frac{\pi}{3} + 2\alpha\right) \right)} = 37.4 \text{ V}$$

$$FF = \frac{V_{RMS}}{V_{DC}} = 1.08$$

$$RF = \sqrt{(FF^2 - 1)} = 0.407$$

$$TUF = \frac{P_{DC}}{3 * V_s * I_s} = 0.149$$

When comparing theoretical calculations to measured values, discrepancies arise. The theoretical Root Mean Square voltage (V_{rms}) was computed to be 37.4 V, while the measured value stood at 41.3 V. The theoretical Direct current voltage (V_{dc}) was determined as 34.5 V, whereas the measured value was 35.1 V. The Form Factor (FF) computed theoretically was 1.08, contrasting with the measured value of 1.18. The Ripple Factor (RF) was theoretically calculated at 0.407, while the measured value was notably higher at 0.620. Additionally, the Total Utilization Factor (TUF) was theoretically 0.149, but the measured TUF was approximately 0.408. These differences suggest potential discrepancies between the theoretical model and real-world observations, indicating the presence of factors not accounted for in the theoretical calculations.

ii. Three-Phase Half-wave Converter with Resistive Load when delay angle =90

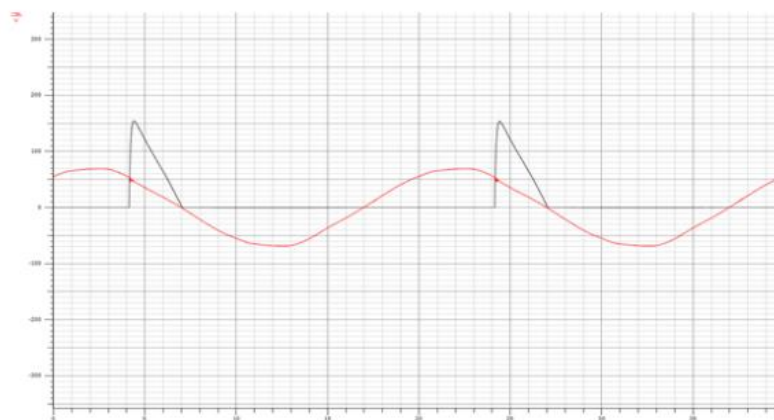


Figure 13: The voltage input and current input when delay angle =90

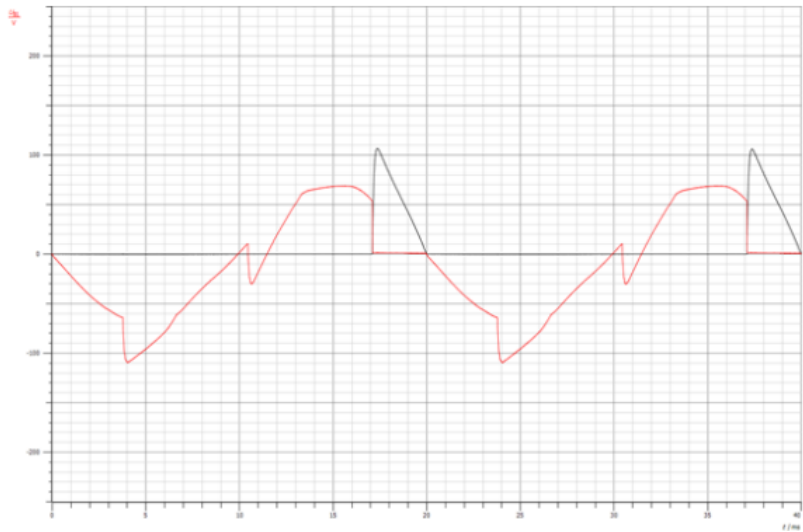


Figure 14: The voltage on SCR with input current

Note: this figures from past report because they didn't take it in our experiment

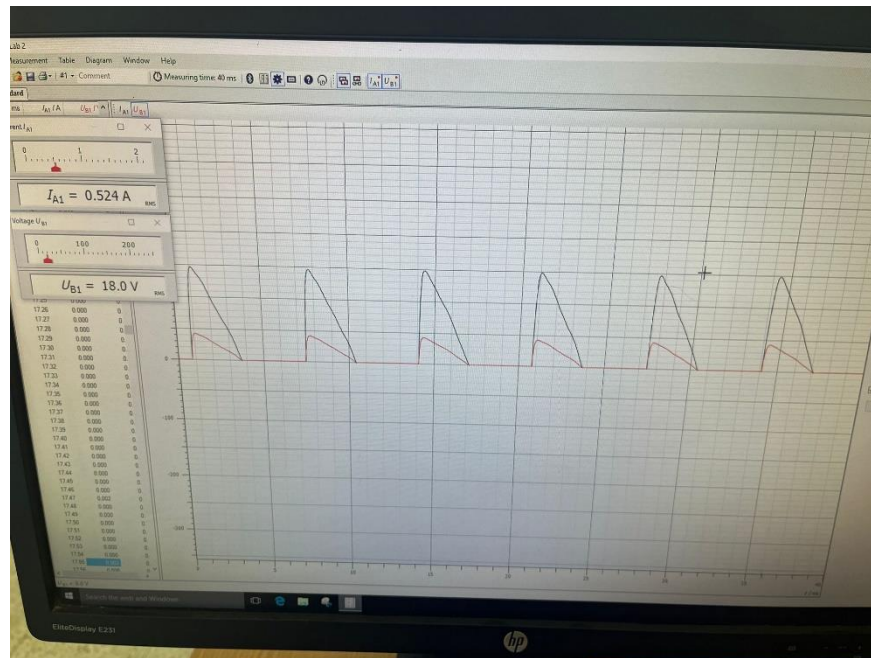


Figure 15: The RMS output voltage and output current when delay angle =90

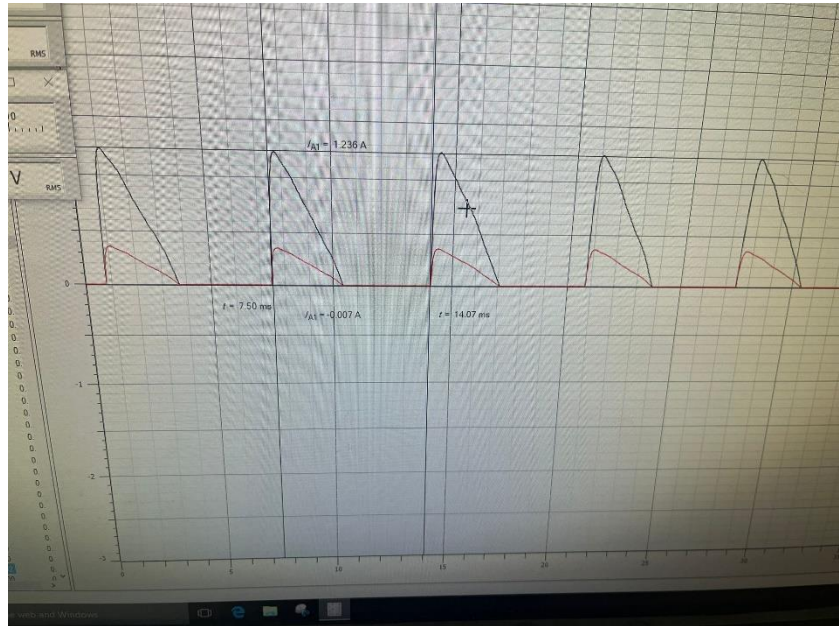


Figure 16: The frequency of the output voltage when delay angle = 90

$$f = \frac{1}{T} = 152.20 \text{ Hz}$$

Equation 16: The Frequency Formula

$$T = T_2 - T_1 = 6.57 \text{ ms}$$

Equation 17: The difference between the two time periods

The provided Figures describe the operation of a three-phase half-wave controlled rectifier with a resistive load and a firing angle of 90 degrees. The average input voltage is approximately 51.7 V, with an input current of around 0.097 A, indicating a relatively stable input. However, the output voltage averages around 10.4 V, significantly lower than the input voltage, which is expected due to rectification. The output current, averaging 0.29 A, is slightly lower than the input current, suggesting some losses in the system. The firing angle of 90 degrees indicates that the thyristors are triggered at the midpoint of each half-cycle of the input voltage waveform. Overall, the rectifier functions in a half-wave mode, converting AC input voltage into pulsating DC output suitable for a resistive load, but further analysis may be needed for optimization. When comparing delay angles in a controlled rectifier, a delay angle of 45° initiates thyristor conduction 45° after each phase's zero crossing, leading to wider rectified voltage pulses and a higher average DC output voltage. Conversely, a delay angle of 90° triggers thyristor conduction 90° after zero crossing, yielding narrower pulses and a lower average DC output voltage. Despite this, the output

waveform exhibits a more pronounced ripple due to the shorter conduction period, resulting in a higher RMS output voltage compared to a 45° delay angle. Ultimately, the choice between delay angles involves trade-offs in output quality and efficiency, impacting average voltage, ripple magnitude, and RMS value.

$$FF = \frac{V_{RMS}}{V_{DC}}$$

Equation 18: The Form Factor

$$FF = \frac{V_{RMS}}{V_{DC}} = 1.75$$

$$RF = \sqrt{(FF^2 - 1)} = 1.43$$

Equation 19: The Ripple Factor

$$TUF = \frac{P_{DC}}{3 * V_s * I_s} = 0.03$$

Equation 20: The Transformer Unitization Factor

$V_m = 45$ V phase to neutral

$\alpha = 90^\circ$

$$V_{dc} = \frac{3V_m}{2\pi} \left(1 + \cos \left(\frac{\pi}{6} + \alpha \right) \right) = 11.51V$$

$$V_{rms} = \sqrt{3} V_m \sqrt{\left(\frac{5}{24} - \frac{\alpha}{4\pi} + \frac{1}{8\pi} \sin \left(\frac{\pi}{3} + 2\alpha \right) \right)} = 11.94 V$$

$$FF = \frac{V_{RMS}}{V_{DC}} = 1.73$$

$$RF = \sqrt{(FF^2 - 1)} = 1.4$$

$$TUF = \frac{P_{DC}}{V_s * I_s} = 0.17$$

In an ideal rectifier scenario, where efficiency (η) is 100%, Form Factor (FF) is 100%, Ripple Factor (RF) is 0%, Total Utilization Factor (TUF) is 100%, Total Harmonic Distortion (THD) is 0%, and Power Factor (PF) as well as Displacement Power Factor (DPF) are both 1, theoretical calculations based on ($V_m = 45$) V phase to neutral and ($\alpha = 90^\circ$) yield values for (V_{dc}) of approximately 11.51 V and (V_{rms}) of approximately 11.94 V. Consequently, the calculated FF is approximately 1.037, RF is approximately 0.27, and TUF is approximately 0.027. However, the measured data reveals different values: FF is approximately 1.75, RF is approximately 1.43, and TUF is approximately 0.316. These disparities between theoretical and measured values suggest deviations from the idealized model, potentially due to non-idealities such as voltage drops, circuit losses, or inaccuracies in measurements. Additionally, the significantly higher FF and RF values indicate greater distortion and ripple in the measured waveform compared to the theoretical predictions.

Table 1: The effect of the delay angle on the average value of output voltage and current of a Three-Phase Half-Wave

Delay angle (α°)	0°	30°	60°	90°	120°	150°
The measured average output voltage ($u_d(\alpha)$) [V]	48.5	39	24.1	10.7	2.1	0
The measured average output current ($i_d(\alpha)$) [A]	1.425	1.151	0.721	0.306	0.057	0
Normalized measured average output voltage, $u_d(\alpha) / u_d(\alpha=0^\circ)$	1	0.804	0.496	0.220	0.04	0
Normalized measured average output current $i_d(\alpha) / i_d(\alpha=0^\circ)$	1	0.807	0.505	0.214	0.04	0
Calculated (theoretical) average output voltage [V]	54.7	45.3	30	15.1	2	0
Normalized theoretical average output voltage, $u_d(\alpha) / u_d(\alpha=0^\circ)$	1	0.82	0.54	0.27	0.03	0

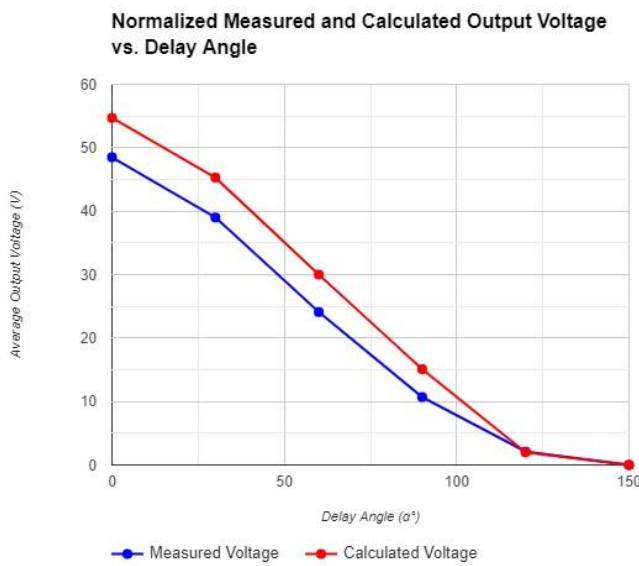


Figure 17: Normalized Measured and Calculated Output Voltage

From the provided data and Figure 17 the curve and observations, it's evident that there's a close correspondence between the theoretical and experimental values of the average output voltage across different delay angles in the electrical circuit. Looking at the comparison table, we see that the theoretical voltages tend to slightly exceed the experimental measurements. This discrepancy can be attributed to the inherent complexities and imperfections present in real-world electrical systems. Theoretical models, while

valuable for understanding system behavior, often assume idealized conditions and component characteristics. In contrast, practical experiments operate within the context of real-world constraints, such as component tolerances, environmental influences, and measurement limitations. These factors collectively contribute to the observed quantitative differences between theoretical predictions and experimental results. Nonetheless, despite these disparities, it's noteworthy that the general trends depicted by both the theoretical and experimental values align closely.

b. Three-Phase Half-wave Converter with Resistive-inductive Load

i. *Three-Phase Half-wave Converter with Resistive-inductive Load and delay angle =45*

The connection was established as shown in Figure 18, particularly with the load RL consisting of three resistors in parallel, each having a resistance of 100Ω , and a $50mH$ inductive component in series. Additionally, it was ensured that the Transformer's secondaries produced a phase-to-neutral voltage of $45V$. Initially, the CASSY probes were connected to plot and measure the input voltage (us_01) and the input current (is) using the CASSY LAB software. The Converter Control Unit (Cat. No. 735 122) was adjusted to produce a delay angle of 45° . The Transformer Supply Voltage Cat. No. 726 80 was turned on, and traces of the input voltage (us_01) and the input current (is) were plotted, with screen shots taken of these plots. Furthermore, the rms value of the input voltage (us_01), and the rms and average values of the input current (is) were measured using the CASSY LAB software. Subsequently, the Transformer Supply Voltage Cat. No. 726 80 was turned off. The voltage probe of CASSY was connected to measure and plot the SCR (valve) voltage (uv), while leaving the current probe unchanged. The Transformer Supply Voltage Cat. No. 726 80 was turned on again and then turned off. The probes of CASSY were connected to measure and plot the output voltage (ud) and the output current (id). The output voltage (ud) and the output current (id) were plotted, with screenshots taken of these plots. Finally, the average and rms values of the output voltage (ud) and the output current (id) were measured.

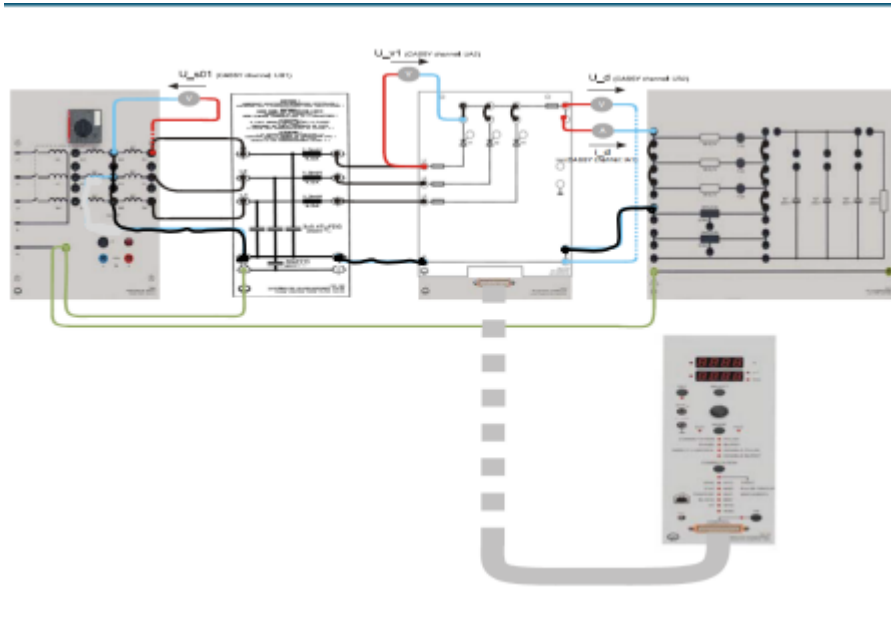


Figure 18: Configuration of Three-Phase Half-Wave Converter supplying a Resistive - Inductive load of 33.3Ω & $50mH$

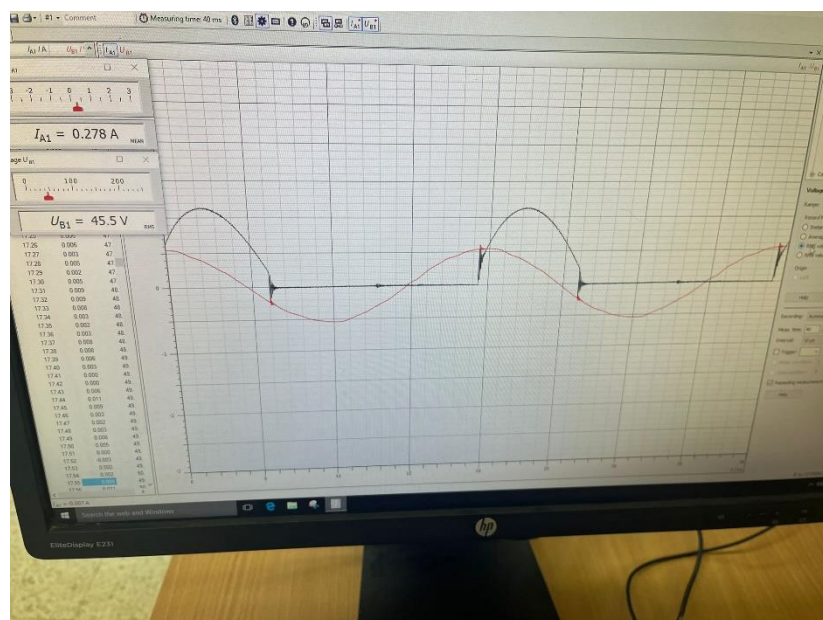


Figure 19: The RMS input voltage and the input current when $\alpha = 45$ in SemiConverter with RL

$$I_{RMS} = \sqrt{2} * I_{AvG}$$

Figure 20: The relationship between the RMS (Root Mean Square) and average values of a waveform

$$I_{RMS} = \sqrt{2} * 0.278 = 0.393$$

Upon realizing the error in measuring current as mean average rather than RMS in the three-phase controlled rectifier setup with an RL load, corrective steps were taken to estimate the RMS value. Applying the formula $I_{RMS} = \sqrt{2} * I_{AVG}$ (where I_{AVG} is the average current) yielded an approximate value of 0.393. However, variations may occur due to complexities like parallel resistors in the load (each 100Ω , with $50mH$) and kit-related factors. While this approximation provides insight, careful interpretation is advised, acknowledging potential disparities in experimental outcomes.

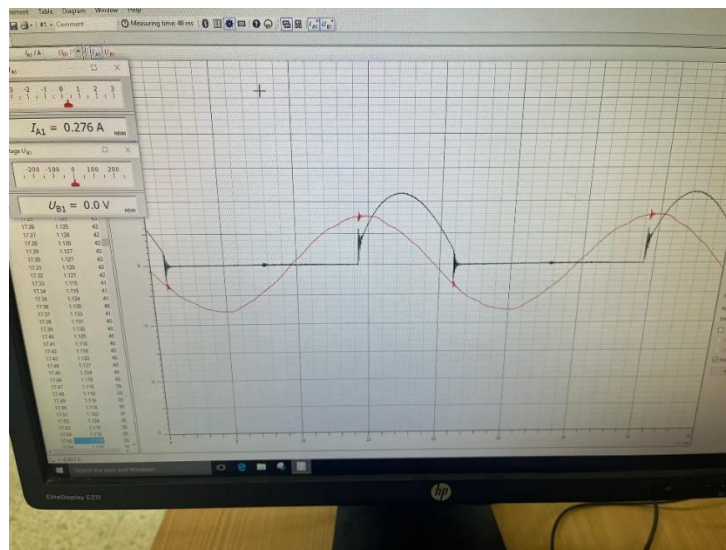


Figure 21: The mean of the input voltage and current for delay angle =45

-UB1: The Input Voltage

-IA1: The Input Current

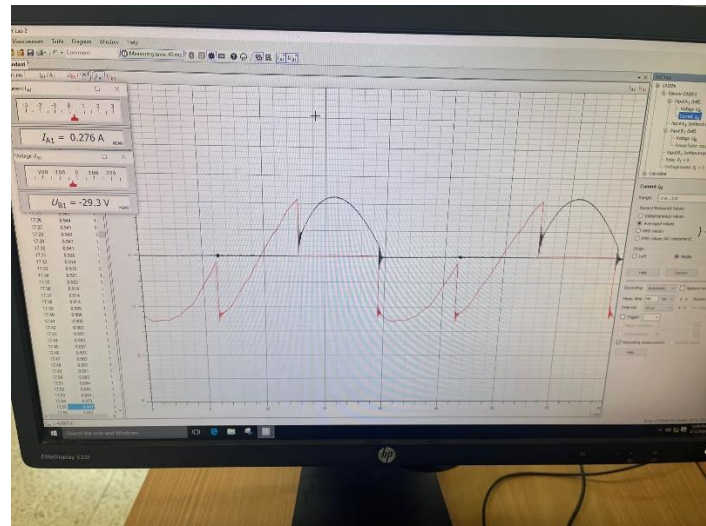


Figure 22: The SCR voltage (UV) and the input current (is) when $\alpha = 45$ in Half-Wave Converter with RL

-UB1: The Output Voltage of SCR

-IA1: The Input Current

In Figure 22, we see the value voltage showing up alongside the source current in both positive and negative parts. This happens because of how the inductor works. It stores some of the current and then lets it out slowly. First, the current goes up steadily until it hits a certain point, then it goes down to zero. After that, the inductor starts working again, releasing the stored current until the load is done. This back-and-forth process shows how the inductor stores and releases energy, which we can see in the waveform.

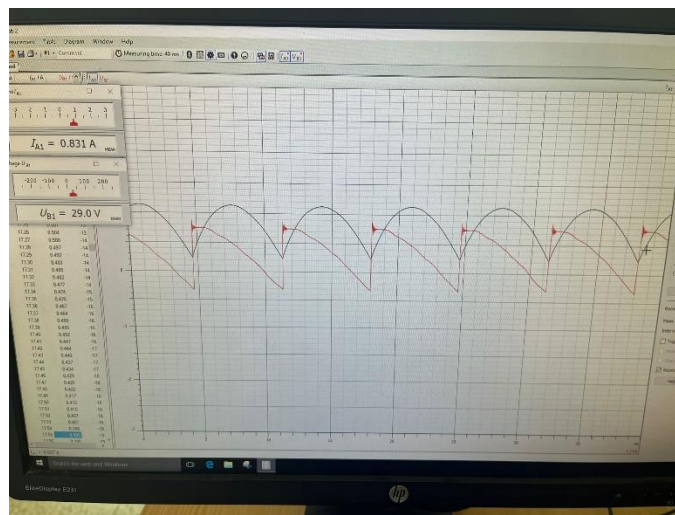


Figure 23: The output voltage and current in the average value of dealy angle = 45

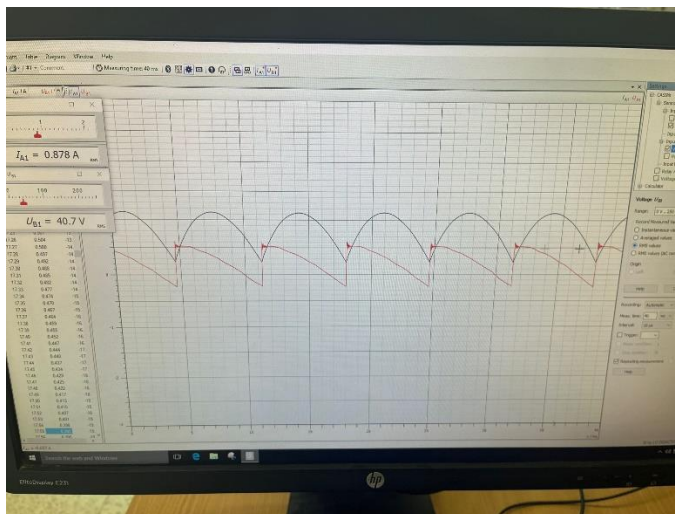


Figure 24: The Output voltage and current in RMS value in dealy angle=45

-UB1: The Output Voltage

-IA1: The Output Current

Table 2: The Values of The output of Three phase half wave controlled rectifier with RL and dealy angle =45

	<i>Output voltage</i>	<i>Output Current</i>
RMS values	40.7	0.878
Average Values	29.0	0.831

$V_m = 45 \text{ V}$ phase to neutral
 $\alpha = 45^\circ$

$$FF = \frac{V_{RMS}}{V_{DC}}$$

Equation 21: The Form Factor

$$FF = \frac{V_{RMS}}{V_{DC}} = \frac{40.7}{29.0} = 1.40$$

$$RF = \sqrt{(FF^2 - 1)} = 0.979$$

Equation 22: The Ripple Factor

$$TUF = \frac{P_{DC}}{V_s * I_s} = 0.991$$

Equation 23: The Transformer Utilization Factor

ii. Three-Phase Half-wave Converter with Resistive Load and delay angle =90

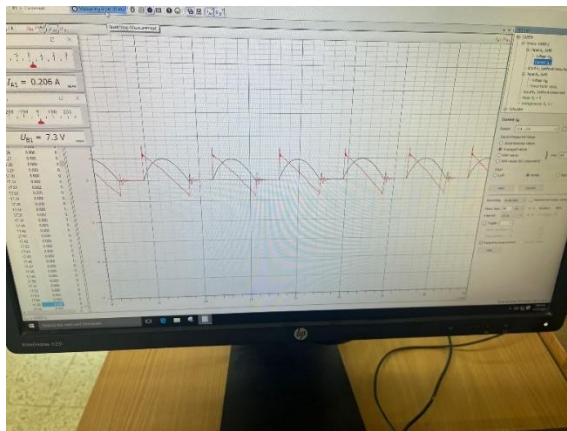


Figure 25: The average output voltage and current of delay angle =90

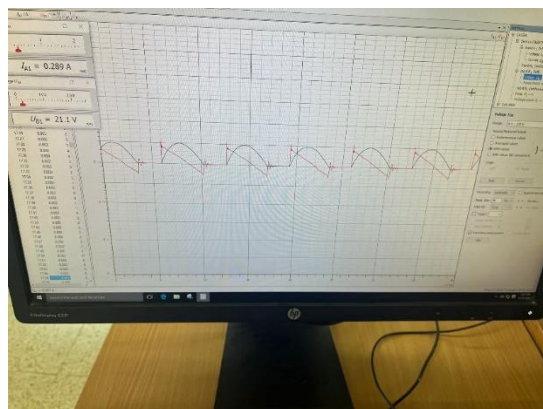


Figure 26: The RMS output voltage of delay angle 90

-UB1: The Output Voltage

-IA1: The Output Current

Table 3: The output voltage of delay angle =90

	<i>Output voltage</i>	<i>Output Current</i>
RMS values	21.1	0.289
Average Values	7.3	0.206

When comparing the output characteristics of the Three-Phase Half-Wave Converter with Resistive-Inductive (RL) Load at different delay angles, notable differences emerge. At a delay angle of 90 degrees, the RMS output voltage is measured at 21.1 volts, with an accompanying current of 0.289. In contrast, shifting the delay angle to 45 degrees results in a substantial increase in both voltage and current, with RMS values of 40.7 volts and 0.878 respectively. This alteration in delay angle significantly impacts the converter's performance, leading to higher output voltages and currents. Such variations highlight the dynamic nature of the converter's operation, underscoring the importance of precise control and

optimization to achieve desired output characteristics.

$$V_m = 45 \text{ V phase to neutral}$$

$$\alpha = 90^\circ$$

$$FF = \frac{V_{RMS}}{V_{DC}} = 2.89$$

$$RF = \sqrt{(FF^2 - 1)} = 2.71$$

Equation 24: The Ripple Factor

$$TUF = \frac{P_{DC}}{3 * V_s * I_s} = 0.095$$

Equation 25: The Transformer Utilization Factor

At delay angles of 90 and 45 degrees in the Three-Phase Half-Wave Converter with a Resistive-Inductive (RL) Load, notable differences in performance metrics are observed. At a delay angle of 90 degrees, the system exhibits lower RMS output voltage and current values (21.1V and 0.289A, respectively) compared to the values at a 45-degree delay angle (40.7V and 0.878A). This decrease in RMS values suggests reduced power delivery to the load when the delay angle is increased. Simultaneously, the average output voltage and current at a 90-degree delay angle (7.3V and 0.206A) are also lower than those at a 45-degree delay angle (29.0V and 0.831A). This reduction in average values further indicates diminished power transfer efficiency at higher delay angles. Regarding waveform distortion, the Form Factor (FF) at a 45-degree delay angle indicates noticeable distortion (140%), while at a 90-degree delay angle, the distortion is significantly higher (289%). This suggests a more pronounced deviation from a pure sinusoidal waveform at the higher delay angle. Similarly, the Ripple Factor (RF) at a 45-degree delay angle indicates a relatively minor ripple (97.9%), whereas at a 90-degree delay angle, the ripple is substantially higher (271%). This indicates increased AC component presence in the output voltage waveform at the higher delay angle, leading to a more significant ripple. Furthermore, the Transformer Utilization Factor (TUF) at a 90-degree delay angle is calculated to be 9.5%, indicating inefficient utilization of the transformer's capacity. In contrast, at a 45-degree delay angle, the TUF is 99.1%, signifying highly efficient utilization of the transformer's capacity. This difference underscores the importance of the delay angle in determining system efficiency and highlights the need for further investigation into the reasons behind the observed discrepancies.

B. Three-Phase Semi-Converter

a. Three-Phase Semi-Converter with Resistive Load

i. *Three-Phase Semi-Converter with Resistive Load with delay angle = 45*

The secondaries of the transformers are connected as Y to produce a phase-to-neutral voltage of 45V, and a resistive load of 300Ω (3 resistors in series, each of 100Ω) is utilized. The Mask (Bridge topology) "735 012 – 09 B6HA, B6HK" is employed, and the Pulse form pulse button is activated. Components are connected as depicted in Figure 27, and the input voltage (u_{S1}) and input current (i_S) are plotted/measured using CASSY probes with the assistance of the CASSY LAB software. The Converter Control Unit (Cat. No. 735 122) is adjusted to produce a delay angle of 45° , and subsequently, the Transformer Supply Voltage

Cat. No. 726 80 is switched on. Traces of the input voltage (u_{s1}) and input current (i_s) are plotted, and screenshots are captured accordingly. The RMS values of the input voltage (u_{s1}) and input current (i_s) are measured using the CASSY LAB software. After turning off the Transformer Supply Voltage Cat. No. 726 80, probes are connected to measure/plot SCR1 (valve) voltage (u_{v1}) and SCR1 (valve) current (i_{T1}). Screenshots of SCR1 voltage (u_{v1}) and current (i_{T1}) plots are taken. The Transformer Supply Voltage Cat. No. 726 80 is turned off again, and probes of CASSY are utilized to measure/plot the output voltage (u_d) and output current (i_d). Screenshots of the output voltage (u_d) and output current (i_d) plots are captured. The peak-to-peak ripple at the output voltage is measured before changing the delay angle to 90° . Probes of CASSY are again used to measure/plot the output voltage (u_d) and output current (i_d), with screenshots captured accordingly. The peak-to-peak ripple at the output voltage is measured once more. The average and rms values of the output voltage (u_d) and output current (i_d) are measured. The Converter Control Unit (Cat. No. 735 122) is then adjusted to produce delay angles (α°) ranging from 0° to 150° in 30° steps to fill in Table 2.2. Finally, the Transformer Supply Voltage Cat. No. 726 80 is turned off, maintaining the connections unchanged.

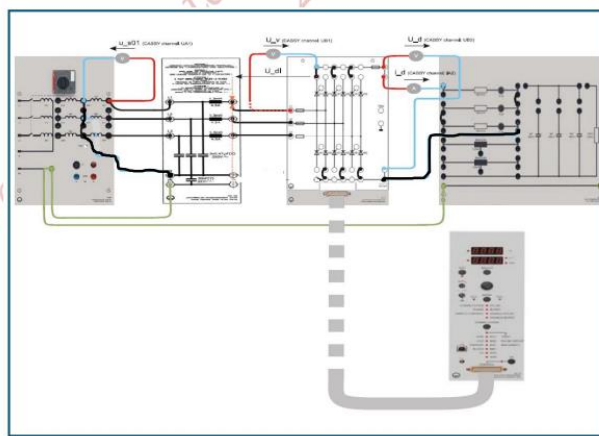


Figure 27: Configuration of Three-Phase Semi-Converter supplying a purely resistive load of 300Ω

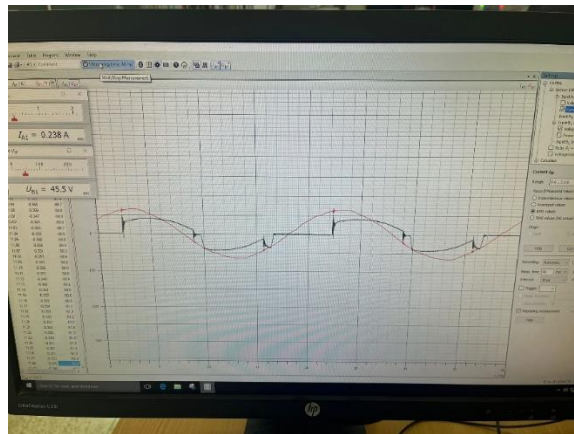


Figure 28: The input voltage (u_{s1}) and the input current (i_s) when $\alpha = 45$ in Semi-Converter with R

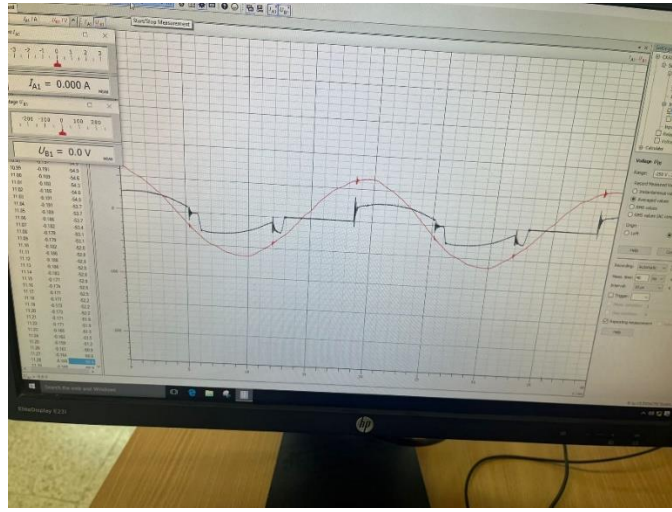


Figure 29: The average input voltage (us01) and the input current (is) when $\alpha = 45$ in Semi-Converter with R

Table 4: The input voltage and current of semi-converter R of delay angle =45

	Input voltage	Input Current
RMS values	45.5	0.238
Average Values	0	0

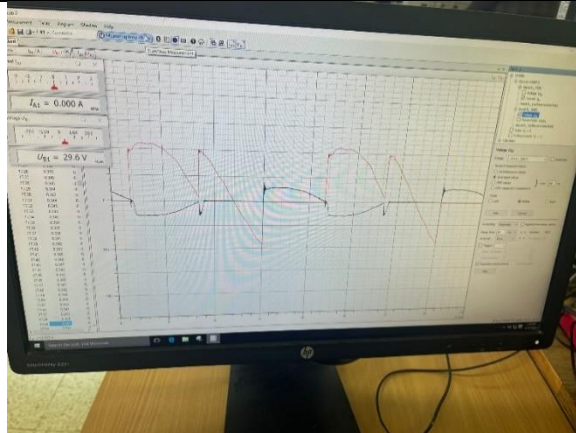


Figure 30: The SCR1 (valve) voltage and SCR1 (valve) current when $\alpha = 45$ in Semi-Converter with R

-UB1: The Output Voltage of SCR

-IA1: The Input Current

In Figure 30, when the delay angle(α) is set to 45 degrees in the Semi-Converter with an added diode, we observe distinct characteristics in the voltage and current of SCR1 (valve). The current through SCR1 flows solely during the positive period, indicating its operation is limited to the positive half cycle. In contrast, the voltage across SCR1 demonstrates activity across both positive and negative periods. This discrepancy in behavior stems from the valve's operational dynamics: during its off state, it behaves akin to an open circuit, permitting voltage flow only during the positive period. However, as the delay angle approaches, SCR1 transitions to a closed state, enabling current flow during the subsequent negative period as well. This phenomenon, commonly referred to as self-switching, underscores the dynamic nature of the valve, as it alternates between open and closed states to facilitate current conduction during specific intervals of the cycle.

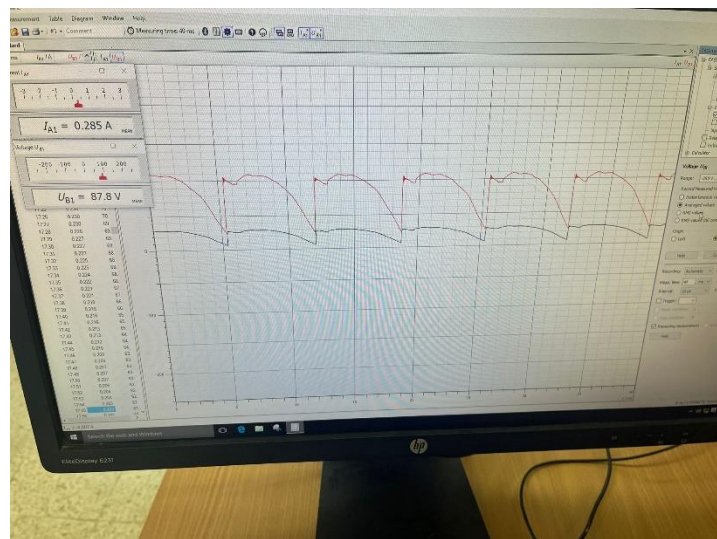


Figure 31 :The average output voltage and the output current when $\alpha = 45$ in Semi-Converter with R

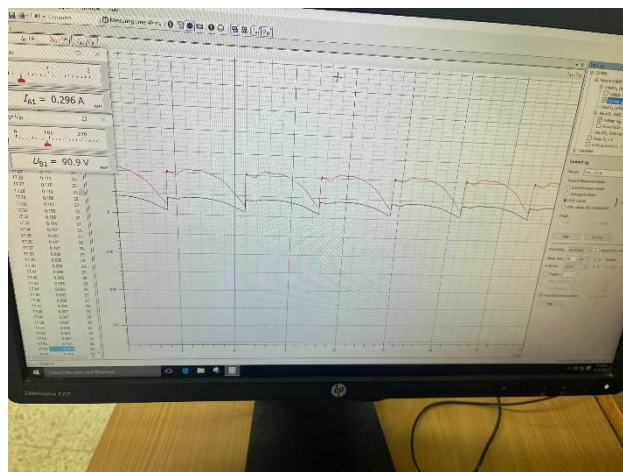


Figure 32: The RMS of the output voltage and the output current when $\alpha = 45^\circ$ in Semi-Converter with R

-UB1: The Output Voltage

-IA1: The Output Current

Table 5: The Output voltage of the Semi-converter of dealy angle=45 with R

	Output voltage	Output Current
RMS values	90.9	0.296
Average Values	87.8	0.285

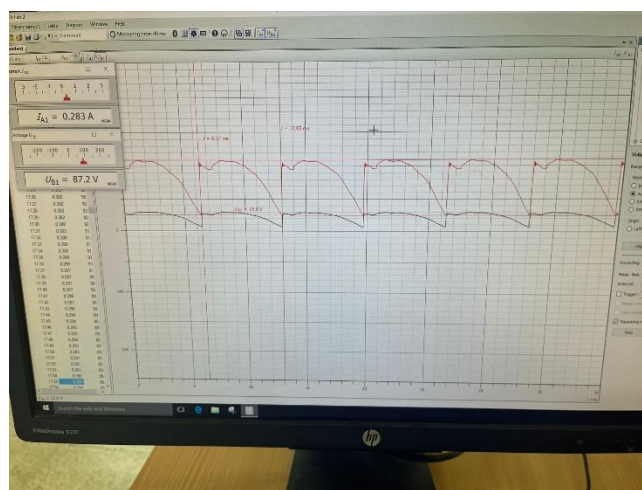


Figure 33: The frequency of the output voltage

$$f = \frac{1}{T} = 150.15 \text{ Hz}$$

Equation 26: The Frequency Formula

$$T = T_2 - T_1 = 6.66\text{ms}$$

Equation 27: The difference between the two time periods

$V_m = 45 \text{ V}$ phase to neutral

$\alpha = 45^\circ$

$$FF = \frac{V_{RMS}}{V_{DC}}$$

Equation 28: The Form Factor

$$FF = \frac{V_{RMS}}{V_{DC}} = \frac{40.7}{29.0} = 1.03$$

$$RF = \sqrt{(FF^2 - 1)} = 0.268$$

Equation 29: The Ripple Factor

$$TUF = \frac{P_{DC}}{V_s * I_s} = 1.96$$

Equation 30: The Transformer Unitization Factor

$$V_{dc} = \frac{3\sqrt{3}V_m}{2\pi} (1 + \cos \alpha) = 64.5$$

$$\text{When } \alpha \leq \frac{\pi}{3} \\ v_{rms} = \sqrt{3} v_m \sqrt{\frac{3}{4\pi} \left(\frac{2\pi}{3} + \sqrt{3} (\cos \alpha)^2 \right)} = 65.5$$

$$FF = \frac{V_{RMS}}{V_{DC}}$$

Equation 31: The Form Factor

$$FF = \frac{V_{RMS}}{V_{DC}} = \frac{40.7}{29.0} = 1.064$$

$$RF = \sqrt{(FF^2 - 1)} = 0.36$$

Equation 32: The Ripple Factor

$$TUF = \frac{P_{DC}}{V_s * I_s} = 3.7$$

Equation 33: The Transformer Unitization Factor

ii. Three-Phase Semi-Converter with Resistive Load with dealy angle =90

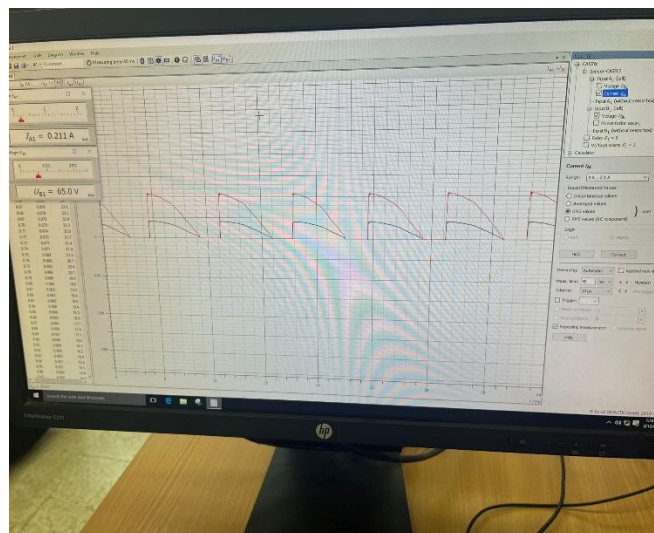


Figure 34: The RMS of the output voltage and the output current when $\alpha = 90$ in Semi-Converter with R

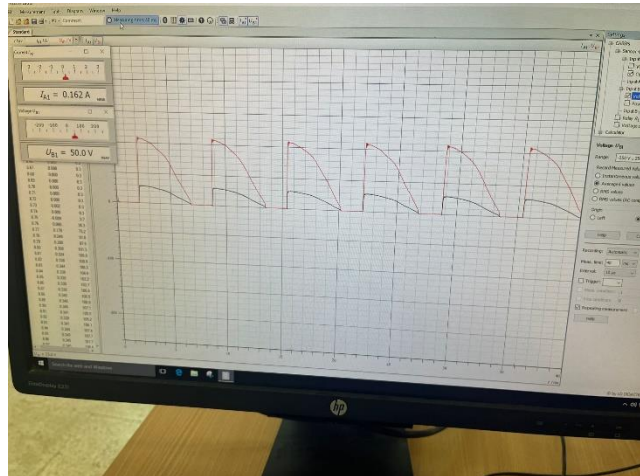


Figure 35: The average of the output voltage and the output current when $\alpha=90$ in Semi-Converter with R

Table 6: The output of the semi-converter with delay angle =90

	<i>Output voltage</i>	<i>Output Current</i>
<i>RMS values</i>	65.0	0.211
<i>Average Values</i>	50	0.162

$$FF = \frac{V_{RMS}}{V_{DC}} = \frac{40.7}{29.0} = 1.3$$

Equation 34: The Form Factor

$$RF = \sqrt{(FF^2 - 1)} = 0.83$$

Equation 35: The Ripple Factor

$$TUF = \frac{P_{DC}}{V_s * I_s} = 0.74$$

Equation 36: The Transformer Unitization Factor

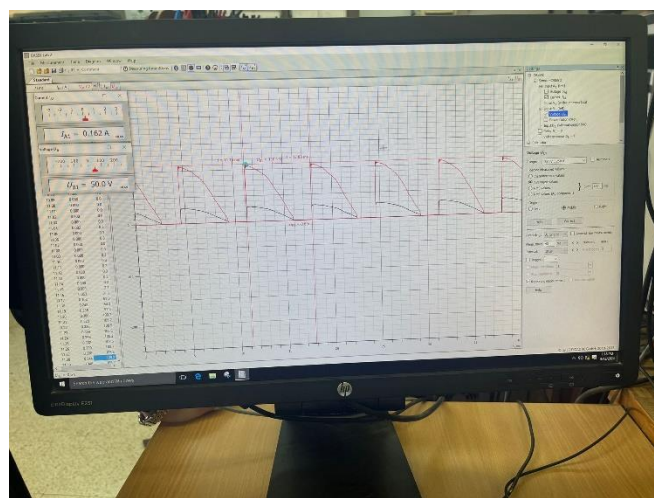


Figure 36: The frequency of the output voltage

$$f = \frac{1}{T} = 149.7 \text{ Hz}$$

Equation 37: The Frequency Formula

$$T = T_2 - T_1 = 6.6 \text{ ms}$$

Equation 38: The difference between the two time periods

Peak – to – peak ripple = Maximum value – Minimum value

Equation 39:the peak-to-peak ripple

$$\text{Peak – to – peak ripple} = 110.1 + 0.6 = 110.7$$

The data presented in Table 6 outlines the output characteristics of the semi-converter with a delay angle set at 90 degrees. Analysis of the provided values reveals notable insights into the performance of the system. Firstly, examining the output voltage and current, we observe a discrepancy between the RMS (Root Mean Square) and average values. The RMS values indicate an output voltage of 65.0 volts and an output current of 0.211 amperes, whereas the average values are slightly lower, with an output voltage of 50 volts and an output current of 0.162 amperes. This disparity suggests potential waveform distortion or non-sinusoidal behavior, as the instantaneous values differ from the average over a complete cycle. Furthermore, the Form Factor (FF) of 1.3 indicates significant waveform distortion. A Form Factor exceeding 1 implies that the peak value of the waveform is higher than expected for a pure sinusoidal waveform, suggesting the presence of harmonic content or distortion. The Ripple Factor (RF) of 0.83 suggests a moderate level of AC ripple present in the output voltage waveform. While not excessively high, it indicates some degree of fluctuation or variation around the average DC value, which may affect the stability or performance of connected loads. Additionally, the Transformer Utilization Factor (TUF) of 0.74 highlights inefficiencies in power delivery. This value indicates that only 74% of the transformer's capacity is effectively utilized to deliver power to the load. Such inefficiencies could arise from mismatches between the transformer rating and the load requirements or suboptimal system design.

Table 7: The effect of the delay angle on the average value of output voltage and current of a Three-Phase

Delay angle (α°)	0°	30°	60°	90°	120°	150°
The measured average output voltage ($u_d(\alpha)$) [V]	102.8	91.5	69.2	42.1	18.3	2.7
The measured average output current ($i_d(\alpha)$) [A]	0.335	0.297	0.225	0.137	0.058	0.009
Normalized measured average output voltage, $u_d(\alpha) / u_d(\alpha=0^\circ)$	1	0.898	0.676	0.409	0.178	0.026
Normalized measured average output current $i_d(\alpha) / i_d(\alpha=0^\circ)$	1	0.886	0.671	0.408	0.173	0
Calculated (theoretical) average output voltage [V]	105	98	77	52	25	7
Normalized theoretical average output voltage, $u_d(\alpha) / u_d(\alpha=0^\circ)$	1	0.933	0.733	0.495	0.238	0.066

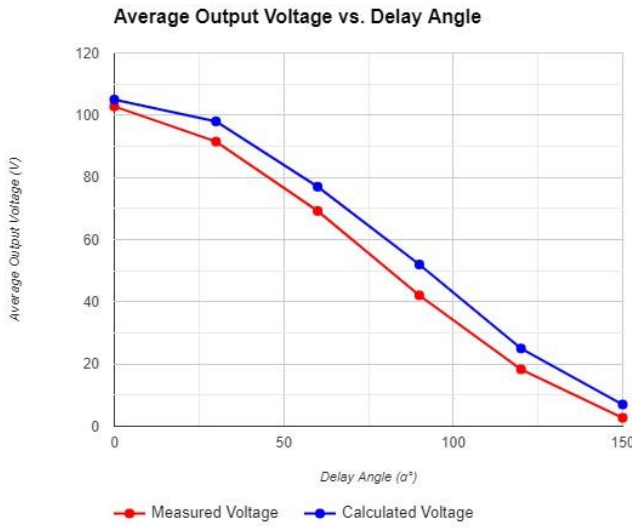


Figure 37: The normalized measured and calculated output voltage as a function of delay angle for a semi-converter with resistive load.

In Figure 37, we observe a notable proximity between the practical and theoretical values, indicating a close alignment in the data. This proximity suggests a high degree of validity in the information obtained from the experimental measurements, reinforcing the reliability of the theoretical model in predicting the system's behavior.

a) Three-Phase Semi-Converter with Resistive-Inductive Load

A. Three-Phase Semi-Converter with Resistive-Inductive Load with delay angle =45

The experiment involves connecting the components as shown in Figure 38. A load resistance of 300Ω (consisting of three resistors in series, each with a value of 100Ω) and an inductance of 50mH (arranged in series) are incorporated. A phase-to-neutral voltage of 45V is ensured from the Transformer's secondaries. Measurements are made using CASSY probes to plot the input voltage ($us01$) and the input current (is) with the CASSY LAB software. The Converter Control Unit (Cat. No. 735 122) is adjusted to achieve a delay angle of 45 degrees. The Transformer Supply Voltage (Cat. No. 726 80) is then activated to facilitate the experiment. Traces of the input voltage ($us01$) and the input current (is) are recorded, and screenshots of these plots are taken for further analysis. RMS values of the input voltage ($us01$) and the input current (is) are determined through the CASSY LAB software. Following this, the Transformer Supply Voltage (Cat. No. 726 80) is deactivated. Continuing the experiment, SCR1 (valve) voltage ($uv1$) and SCR1 (valve) current ($it1$) are measured and plotted using the CASSY probes. Upon reactivation of the Transformer Supply Voltage (Cat. No. 726 80), SCR1 voltage ($uv1$) and current ($it1$) are plotted, and screenshots of these plots are taken. Average and RMS values of the output voltage (ud) and the output current (id) are measured subsequently. Finally, the Transformer Supply Voltage (Cat. No. 726 80) is turned off while maintaining the connections, and the Converter Control Unit (Cat. No. 735 122) is readjusted to achieve a

delay angle of 90 degrees. The experiment is repeated following the same procedure as outlined above.

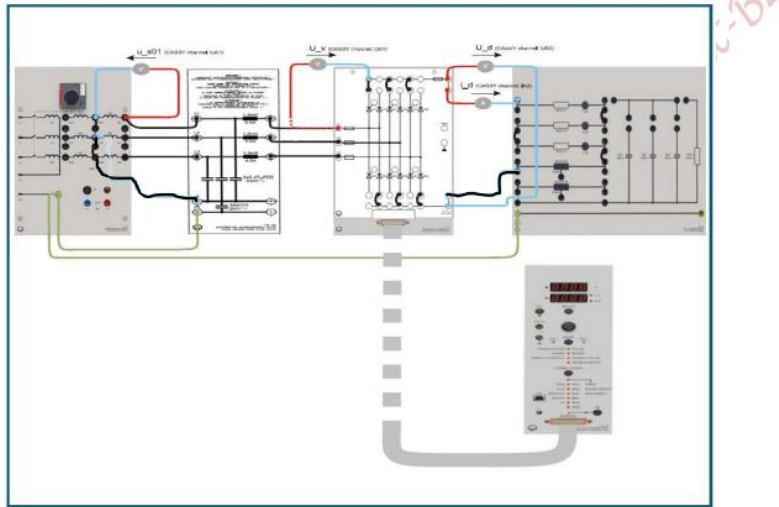


Figure 38: Configuration of Three-Phase Semi-Converter supplying an RL load of 300Ω and $50mH$

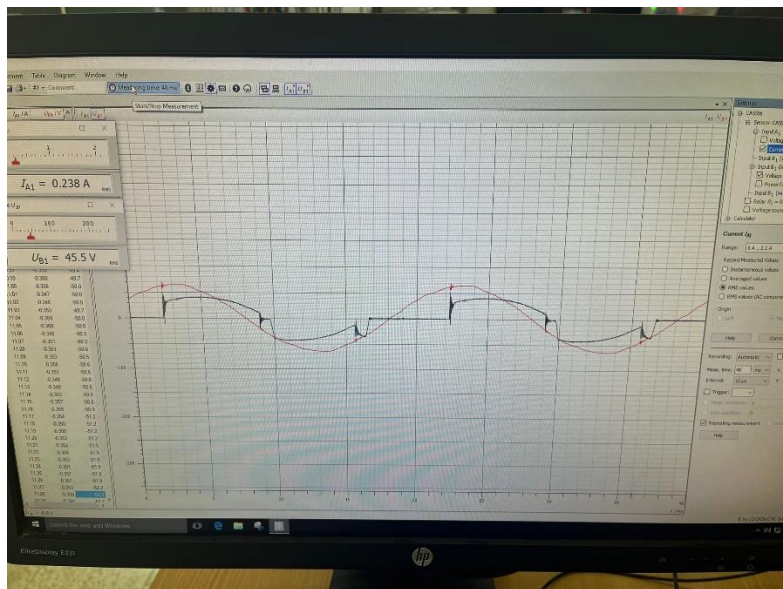


Figure 39: The RMS Input voltage and current of the there phase semi-converter with dealy angle =45

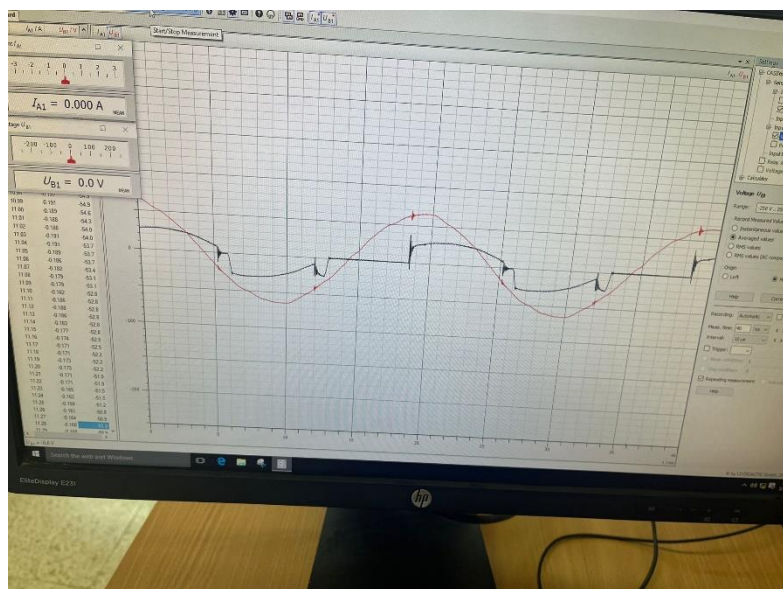


Figure 40: The Average Input voltage and current of the there phase semi-converter with dealy angle =45

In Figures 39 and 40, a subtle delay in the current waveform is evident, attributed to the operational principles of the inductor. Initially, the inductor requires time to store the incoming current before subsequently discharging it, resulting in the observed waveform. This delay reflects the inherent behavior of the inductor in the circuit. Regarding the average current and voltage values, they appear to equate to zero. This equilibrium arises due to the symmetry in the waveform, where the positive and negative parts balance each other out. Consequently, despite fluctuations in the waveform, the net average remains neutral, reinforcing the symmetrical nature of the waveform's behavior.

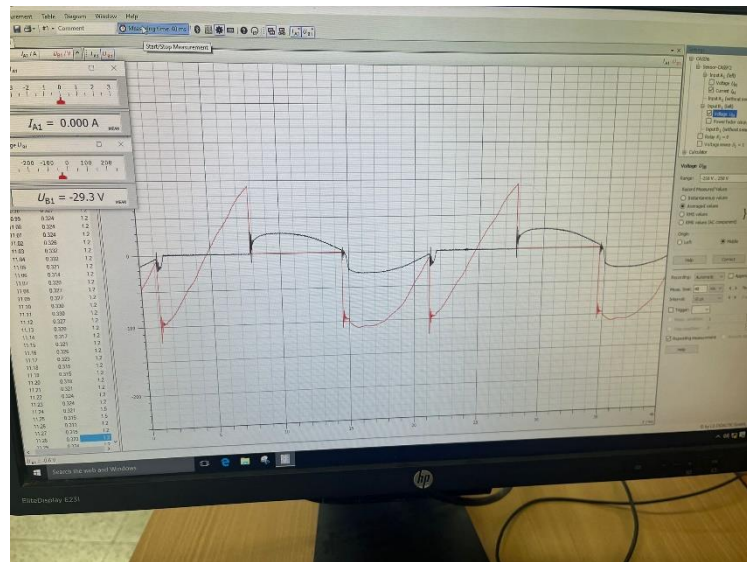


Figure 41: The Average voltage and current of Three-Phase Semi-Converter with Resistive-Inductive Load of dealy angle =45

In Figure 41, the current waveform of a three-phase semi-converter exhibits both positive and negative segments due to the SCR's conduction being limited to 120-degree intervals of the AC cycle. The voltage waveform shows peaks followed by zero voltage intervals, reflecting the SCR's switch-like behavior. During conduction, the SCR presents a minimal voltage drop akin to a closed switch, resulting in nearly zero voltage across it. Conversely, when off, it blocks current, resembling an open circuit and allowing the AC peak voltage to appear across it. The interplay between the SCR's switching action and the AC input voltage yields the characteristic chopped waveform for both current and voltage. Notably, the firing angle dictates the SCR's conduction window, with a larger angle reducing the average output voltage. Additionally, inductive loads can introduce discontinuities in the current waveform, leading to zero current periods even during conduction intervals.

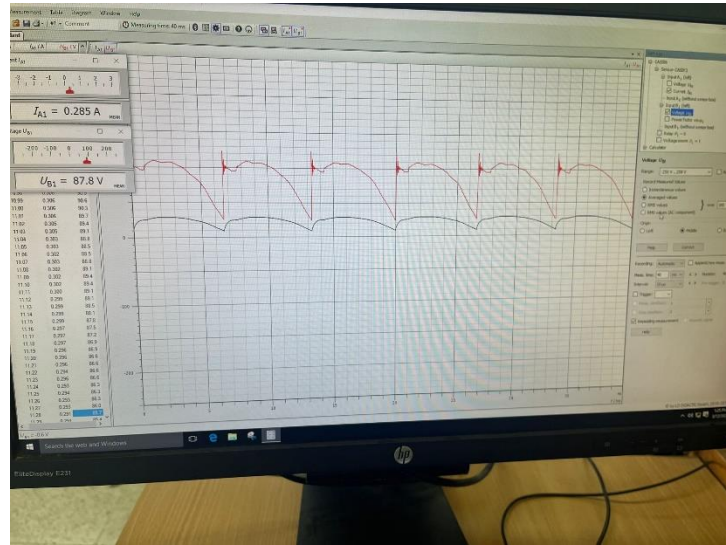


Figure 42: The average output voltage and the output current when $\alpha = 45$ in Semi-Converter with RL

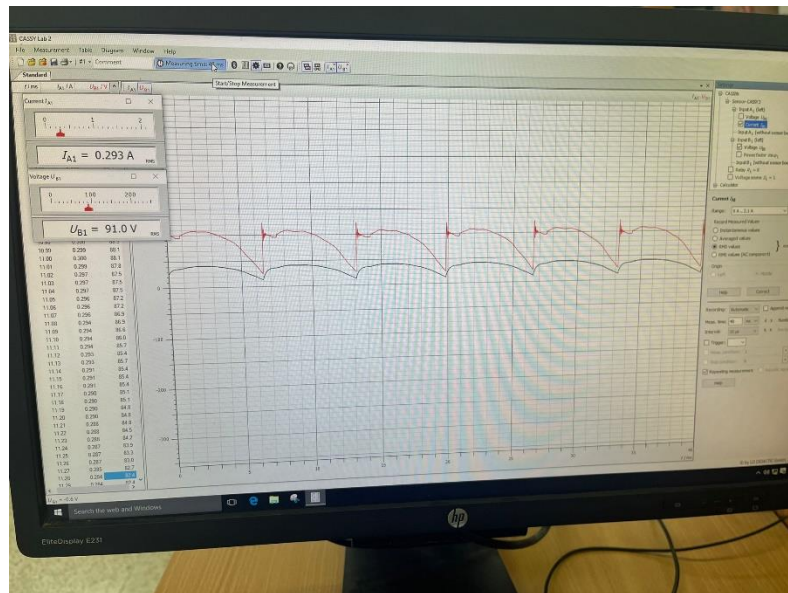


Figure 43: The RMS output voltage and the output current when $\alpha = 45$ in Semi-Converter with RL

Table 7: The Output of Semi-converter with RL and delay angle =45

	<i>Output voltage</i>	<i>Output Current</i>
<i>RMS values</i>	91	0.293
<i>Average Values</i>	87.8	0.285

In Figures 42 and 43, the output characteristics of a three-phase semi-converter with an RL load are depicted, with a firing angle of 45 degrees. Notably, the output voltage exhibits RMS and average values of 91 and 87.8 respectively, while the corresponding current values are 0.293 and 0.285. Interestingly, both the current and voltage waveforms feature only positive half cycles, indicating that conduction occurs solely during one-quarter of the output cycle. This behavior aligns with the operation of a semi-converter, where the SCR conducts during specific intervals determined by the firing angle. In this case, with a 45-degree firing angle, conduction occurs for one-quarter of the cycle. This asymmetrical conduction results in an output waveform characterized by a single positive half cycle, illustrating the unique operation of a three-phase semi-

converter with a resistive-inductive load under these conditions.

The measured RMS output voltage (91V) is very close to the theoretical RMS value (92V), indicating that the theoretical model aligns well with the system's actual performance. Similarly, the measured average output voltage (87.8V) is in good agreement with the theoretical average value (89V), further validating the accuracy of the theoretical calculations. Overall, the close correspondence between the theoretical and measured values suggests that the theoretical model accurately predicts the behavior of the three-phase semi-converter with the given parameters. Any small discrepancies between the theoretical and measured values could be attributed to factors such as component tolerances, circuit losses, or measurement inaccuracies.

B. Three-Phase Semi-Converter with Resistive-Inductive Load with delay angle =90

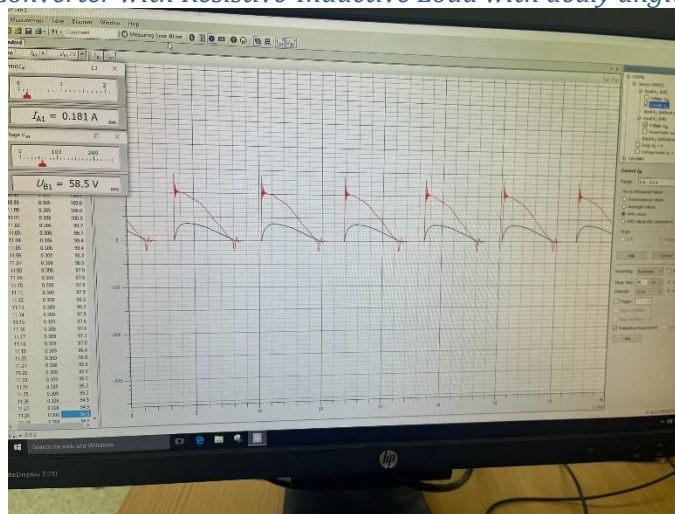


Figure 44: The RMS of the output voltage and current with RL and delay angle =90

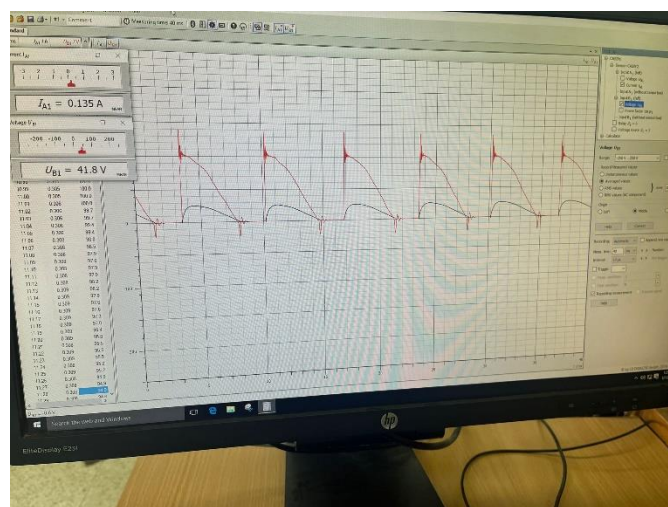


Figure 45: The Average output voltage and current with RL and delay angle =90

Table 8: The Output of Three-phase semi-converter of dealy angle =90 RL

	<i>Output voltage</i>	<i>Output Current</i>
RMS values	58.5	0.181
Average Values	41.8	0.135

The RMS values of the output voltage, calculated at 62 theoretically and measured at 58.5V, demonstrate a close correspondence. Similarly, the average values of 47.3V (theoretical) and 41.8V (measured) also exhibit a notable alignment. This closeness between the calculated and measured values suggests a strong agreement between the theoretical predictions and the practical outcomes of the three-phase semi-converter. Such consistency reinforces the reliability of the theoretical model in accurately estimating the performance parameters of the system under consideration.

Comparing the results between the purely resistive load and the RL (resistive-inductive) load for delay angles of 45° and 90° reveals substantial differences in the waveforms of the output voltage, as well as their average and RMS values. With a purely resistive load, the output voltage waveform remains predominantly positive throughout the cycle, exhibiting minimal distortion. However, with an RL load, especially at a delay angle of 90° , the output voltage waveform may contain negative portions due to the presence of inductance. This results in a more complex waveform shape with potential voltage drops and delays. Additionally, for both delay angles, the average values of the output voltage are higher with the purely resistive load compared to the RL load. This is because the inductive component in the RL load causes voltage drops and delays, resulting in lower average voltage values. Furthermore, RMS values of the output voltage also differ between the purely resistive and RL loads. In general, the RMS values tend to be higher with purely resistive loads compared to RL loads due to the absence of voltage distortions caused by inductance. These differences underscore the significant impact of load type and delay angle considerations on the performance characteristics of three-phase semi-converter.

A. Three-Phase Full-Converter

a) Three-Phase full-Converter with Resistive Load

A. *Three-Phase Full-Converter with Resistive Load with delay angle =45*

Figure 46 depicts the connection of components, featuring a purely resistive load of 300Ω , comprising three resistors in series, each rated at 100Ω . Priority was given to ensuring that the Transformer's secondary produced a phase-to-neutral voltage of 45V. Initially, SCR1 voltage (uv_1) and SCR1 current (iT_1) were monitored using the CASSY probes. The Converter Control Unit (Cat. No. 735 122) was then adjusted to achieve a precise delay angle of 45° . Following this, the activation of the Transformer Supply Voltage, Cat. No. 726 80, led to meticulous capturing and documentation of SCR voltage (uv_1) and current (iT_1) waveforms through screen captures, with subsequent commentary provided to elucidate waveform nuances. Deactivation of the Transformer Supply Voltage left connections intact. Subsequently, the repositioning of CASSY probes facilitated the measurement of output voltage (ud) and output current (id) using the CASSY LAB software. Upon reactivation of the Transformer Supply Voltage, meticulous plotting of output voltage (ud) and output current (id) traces ensued, accompanied by corresponding screen captures. The CASSY

LAB software was then utilized to meticulously measure rms and average values of output voltage (u_d) and output current (i_d), alongside determining the peak-to-peak ripple in output voltage. Deactivation of Transformer Supply Voltage ensued. Next, the Converter Control Unit (Cat. No. 735 122) was fine-tuned to generate a delay angle of 90° . Subsequently, a meticulous exploration of a range of delay angles (α°) from 0° to 150° in 30° increments was undertaken to meticulously populate Table 11 with data. Finally, the reactivation of the Transformer Supply Voltage, Cat. No. 726 80, was carried out to facilitate further experimentation.

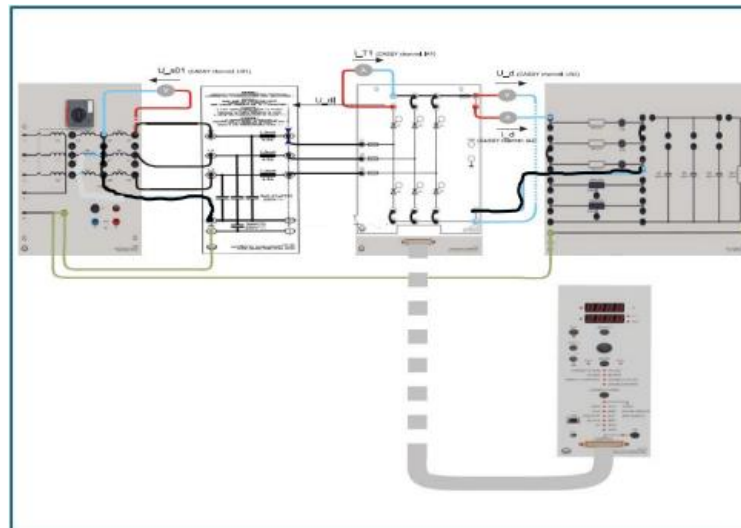


Figure 46: Configuration of Three-Phase Full-Converter supplying a purely resistive load of 300Ω

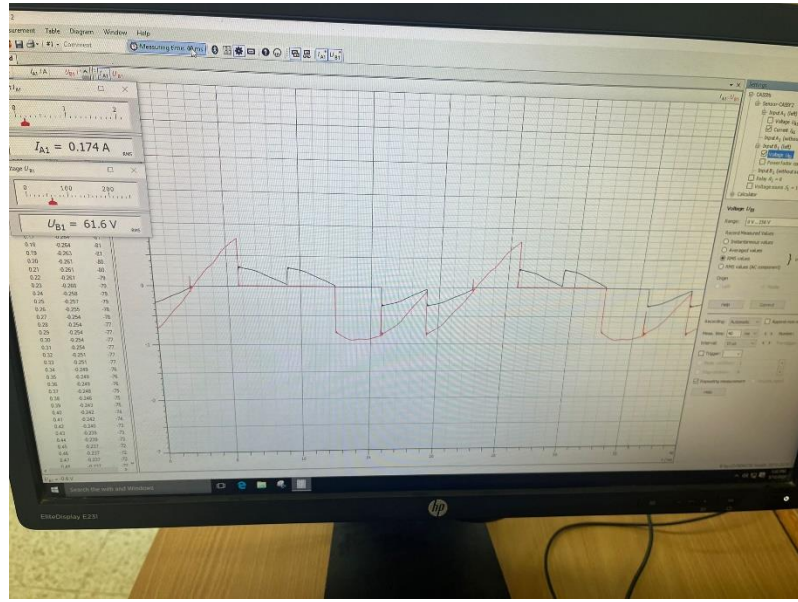


Figure 47: The Voltage and current of the SCR with dealy angle =45 for full-converter with R

At $\alpha = 45^\circ$ in the Full-Converter with a resistive load, the SCR voltage (uv_1) and current (iT_1) exhibit controlled triggering and stable conduction phases, leading to smooth transitions and consistent electricity flow through the circuit. The measured RMS voltage of 61.6V and current of 0.174A validate this behavior, indicating the proper functioning of the converter under these conditions. This observation highlights the critical role of the SCR in regulating voltage and current in the circuit, ensuring stable and efficient power delivery to the load.

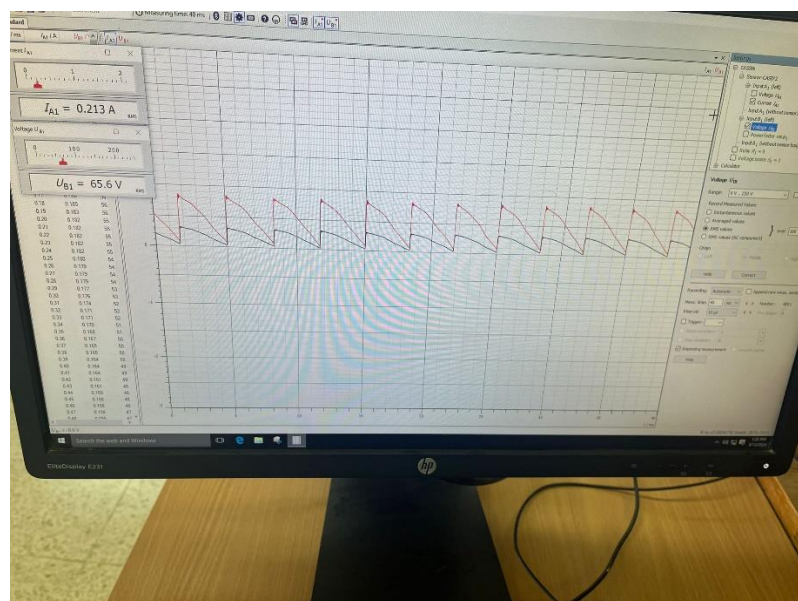


Figure 48: The RMS output voltage of a three-phase full-converter with R of dealy angle =45

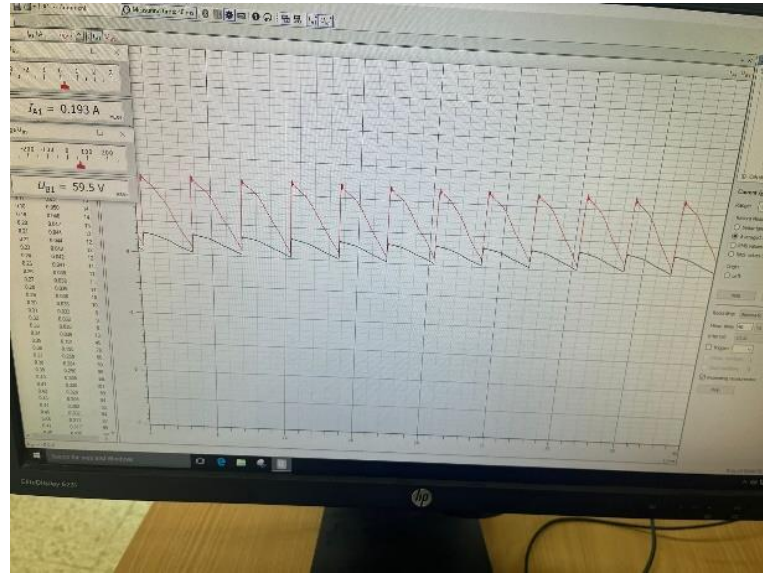


Figure 49: The average output of a three-phase full-converter with R of dealy angle =45

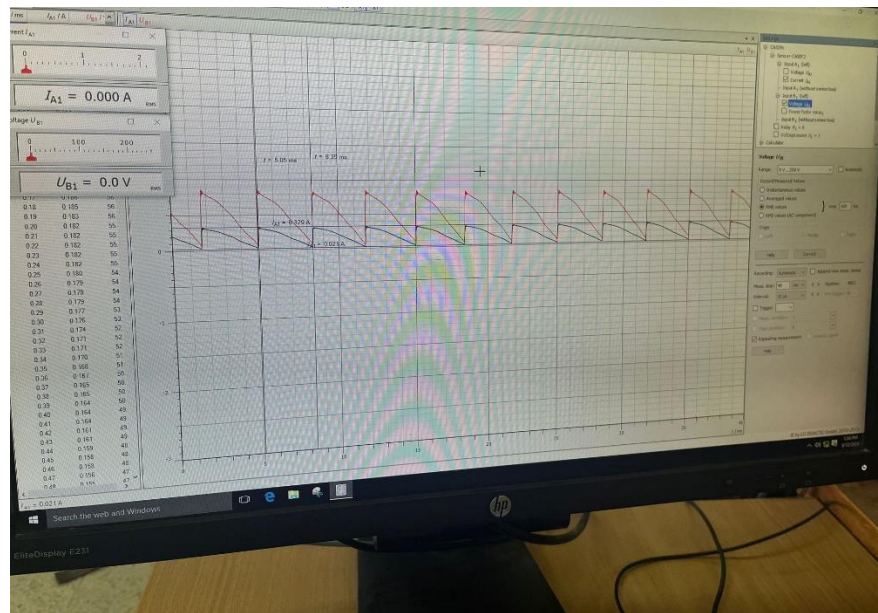


Figure 50: The measured to calculate the frequency of three-phase full-wave converters with dealy angle =45

$$f = \frac{1}{T} = 303.02 \text{ Hz}$$

Equation 40: The Frequency Formula

$$T = T_2 - T_1 = 3.3\text{ms}$$

Equation 41: The difference between the two time periods

Table 9: The Output voltage of a three-phase full converter with delay angle =45

	Output voltage	Output Current
RMS values	65.6	0.213
Average Values	59.5	0.193

$$FF = \frac{V_{RMS}}{V_{DC}} = \frac{40.7}{29.0} = 1.1$$

Equation 42: The Form Factor

$$RF = \sqrt{(FF^2 - 1)} = 0.45$$

Equation 43: The Ripple Factor

$$TUF = \frac{P_{DC}}{V_s * I_s} = 1.70$$

Equation 44: The Transformer Utilization Factor

Table 10: The theoretical value of three-phase full-converter

	<i>Output voltage</i>
RMS values	37.3
Average Values	15

$$FF = \frac{V_{RMS}}{V_{DC}} = \frac{40.7}{29.0} = 2.5$$

Equation 45: The Form Factor

$$RF = \sqrt{(FF^2 - 1)} = 2.29$$

Equation 46: The Ripple Factor

From these values, the Form Factor (FF) and Ripple Factor (RF) are calculated. The Form Factor is computed as the ratio of RMS voltage to DC voltage, yielding a value of 2.26. The Ripple Factor, indicative of waveform distortion, is determined to be 1.97. Additionally, the Transformer Utilization Factor (TUF) is calculated, providing insight into the efficiency of transformer usage. With a TUF of 1.70, the converter appears to be utilizing the transformer effectively. Comparing these results to the theoretical values presented in Table 10, discrepancies arise. Theoretical RMS and average voltages are notably lower at 37.3 volts and 15 volts, respectively. The Form Factor and Ripple Factor are higher at 2.5 and 2.29, respectively. Overall, the analysis suggests that while the three-phase full converter with a 45-degree delay angle is functioning within acceptable parameters, there is a disparity between observed and theoretical values, particularly concerning waveform distortion and transformer utilization. Further investigation may be warranted to optimize converter performance.

Table 11: The normalized measured and calculated output voltage of delay angle=45 for Full-phase converter

Delay angle (α°)	0°	30°	60°	90°	120°	150°

The measured average output voltage ($u_d(\alpha)$) [V]	101.9	79.6	36.9	5.5	0	0
The measured average output current ($i_d(\alpha)$) [A]	0.331	0.259	0.117	0.016	0	0
Normalized measured average output voltage, $u_d(\alpha) / u_d(\alpha=0^\circ)$	1	0.781	0.362	0.220	0.053	0
Normalized measured average output current $i_d(\alpha) / i_d(\alpha=0^\circ)$	1	0.782	0.353	0.048	0	0
Calculated (theoretical) average output voltage [V]	109	94	54	15	0	0
Normalized theoretical average output voltage, $u_d(\alpha) / u_d(\alpha=0^\circ)$	1	0.86	0.49	0.137	0	0

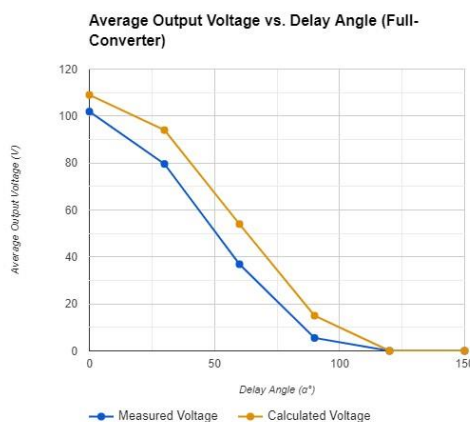


Figure 51: The normalized measured and calculated output voltage as a function of delay angle =45 for Full-phase converter

When comparing the experimental (practical) and theoretical values of the average output voltage across various delay angles (α°) in a power electronic system, differences arise due to real-world factors such as component tolerances and circuit losses. At $\alpha = 0^\circ$, the measured value is slightly lower than the theoretical one, likely due to voltage drops and regulation imperfections. As α increases, larger discrepancies occur, attributed to increased conduction losses and reduced effective voltage during the conduction phase. However, at $\alpha = 90^\circ$, theoretical and measured values align closely, indicating accurate prediction by the theoretical model. At $\alpha = 120^\circ$ and $\alpha = 150^\circ$, both theoretical and measured values are zero, confirming complete blocking of the output voltage. This comparison emphasizes the importance of considering practical factors alongside theoretical calculations in analyzing power electronic system behavior.

B. Three-Phase Full-Converter with Resistive Load with delay angle =90

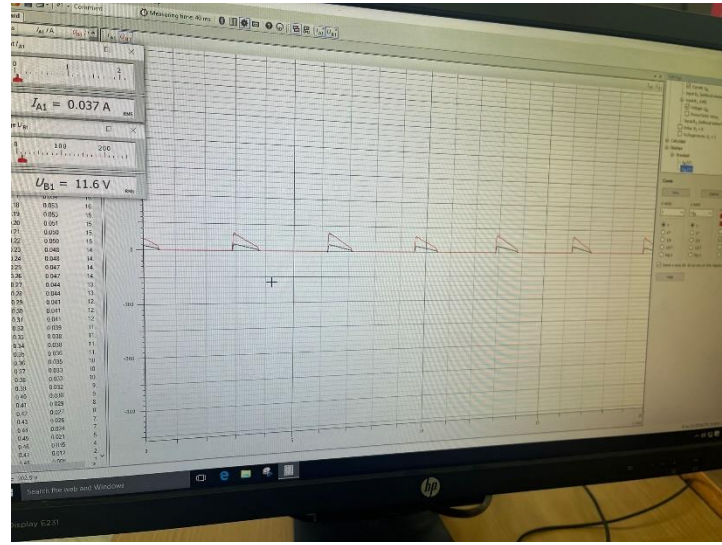


Figure 52: The RMS of the output voltage of a three-phase full-converter with delay angle =90

It's noted that the screen of the average output voltage for the three-phase full converter with resistive load and a delay angle of 90° was not captured. As a result, the form factors (FF), ripple factors (RF), and total utility factors (TUF) for this particular part cannot be determined without this essential data. It's crucial to ensure complete data collection for accurate analysis and evaluation of the converter's performance.

b) Three-phase full-Converter with resistive-Inductive Load

A. Three-Phase Full-Converter with resistive-inductive Load with delay angle =45

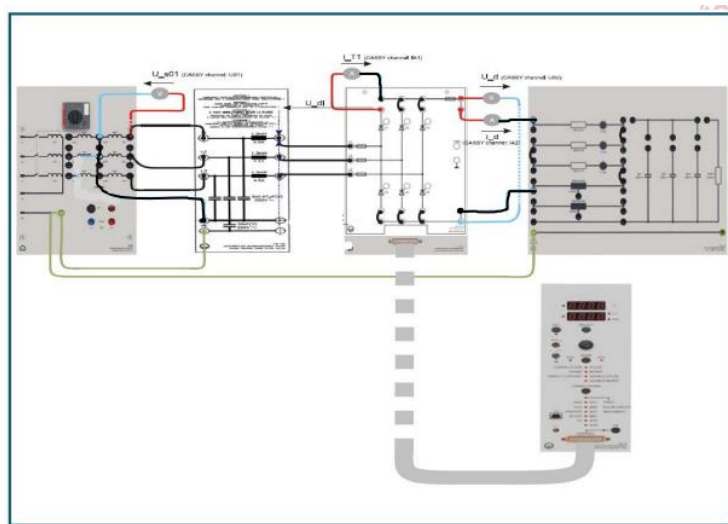


Figure 53: Configuration of Three-Phase Full-Converter supplying an RL load of 300Ω and 50mH

The RL load components were reconnected as depicted in Figure 53, featuring a load resistance of 300Ω (three resistors in series, each with 100Ω) and a series inductance of 50mH. Prioritization was given to ensuring that the Transformer's secondary produced a phase-to-neutral voltage of 45V. Initially, the CASSY probes were connected to measure and plot the input voltage (us01) and input current (is) using the CASSY LAB software. Subsequently, the adjustment of the Converter Control Unit (Cat. No. 735 122) was carried

out to achieve a delay angle of 45° . Upon activation of the Transformer Supply Voltage Cat. No. 726 80, traces of the input voltage (u_{S1}) and input current (i_S) were pscreenshotsscreen shots of these plots were captured. The RMS values of the input voltage (u_{S1}) and input current (i_S) were measured using the CASSY LAB software. Following the deactivation of the Transformer Supply Voltage, the connection of the CASSY probes was adjusted to measure and plot SCR1 (valve) voltage (u_{V1}) and SCR1 (valve) current (i_{T1}). Upon reactivation of the Transformer Supply Voltage, SCR1 voltage (u_{V1}) and current (i_{T1}) waveforms were plotted, and screenshots were taken. Subsequently, the Transformer Supply Voltage was turned off. The CASSY probes were then reconnected to measure and plot the output voltage (u_d) and output current (i_d). Upon reactivation of the Transformer Supply Voltage, the output voltage (u_d) and output current (i_d) waveforms were plotted, and screenshots were taken. The average and rms values of the output voltage (u_d) and output current (i_d) were measured. Commentary on the output voltage and current waveforms was provided, and the connections were maintained as the Transformer Supply Voltage Cat. No. 726 80 was turned off. Subsequently, the adjustment of the Converter Control Unit (Cat. No. 735 122) was carried out to produce a delay angle of 90° .

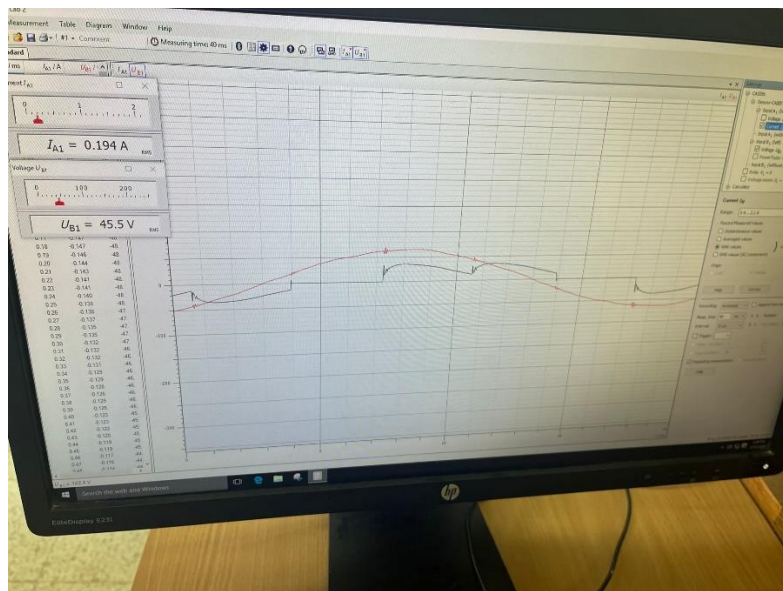


Figure 54: The RMS input voltage and current input of a three-phase full converter with delay angle=45 with RL

Figure 54 illustrates the input voltage and current waveforms. The voltage waveform oscillates between positive and negative phases, reflecting the operation of the full converter. This dynamic arises from the collaboration of two valves within the converter's circuitry. Additionally, it's noteworthy that the average input voltage sums to zero. This balance signifies symmetrical operation within the system, with equal durations of positive and negative voltage. These graphical representations provide valuable insights into the behavior and functionality of the electrical system under scrutiny.

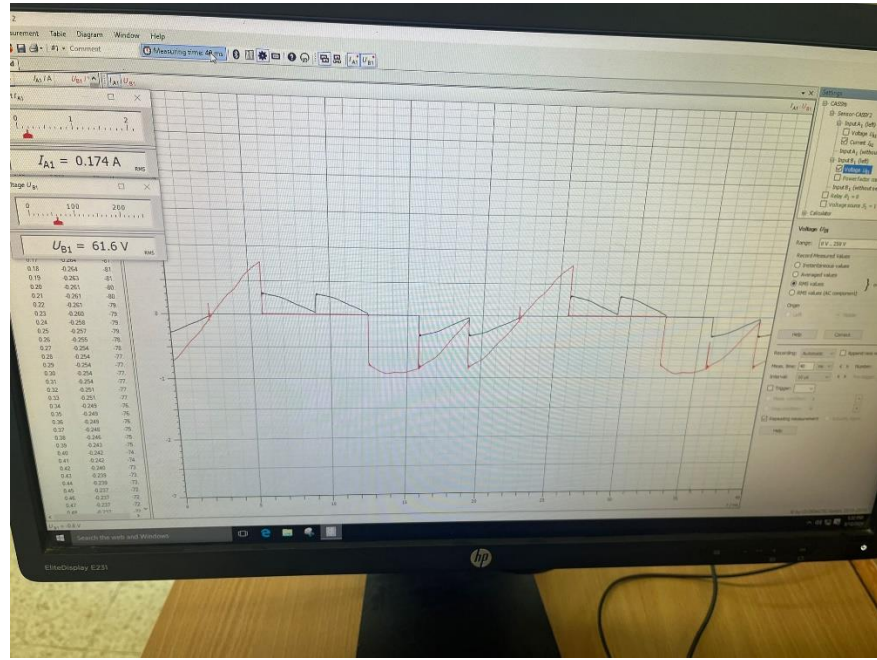


Figure 55: The voltage and current on the SCR of a three-phase full converter with dealy angle =45

In Figure 55, we observe a representation of SCR1 voltage and SCR1 current. Notably, the current in the negative segment is nullified, owing to the operational principles of the full converter. Moreover, we can discern that current initiation occurs following a delay angle of 45 degrees, subsequently reaching zero. Following this, the discharge of the inductor commences, resulting in the emergence of the observed waveform shape in the negative segment, offset by 45 degrees. This depiction provides valuable insights into the behavior and dynamics of the converter system.

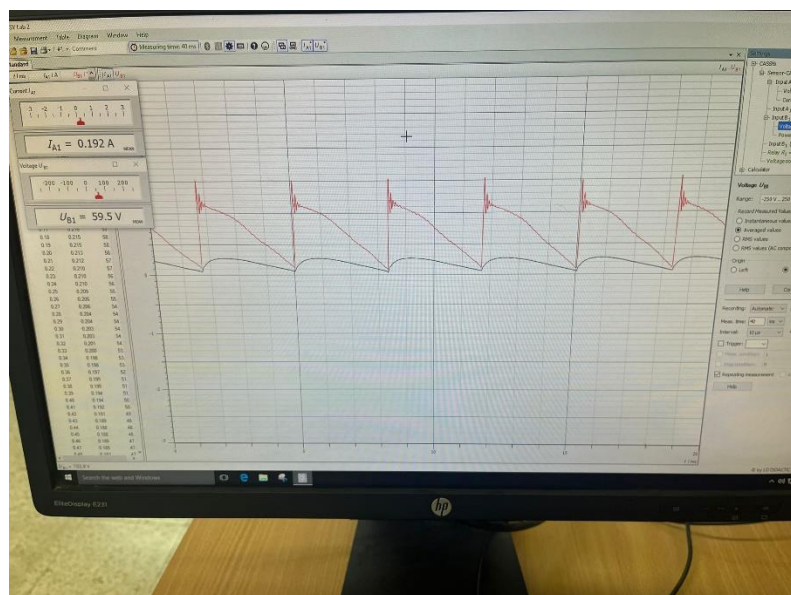


Figure 56: The average Voltage of three phase full conveter with RL & dealy angle =45

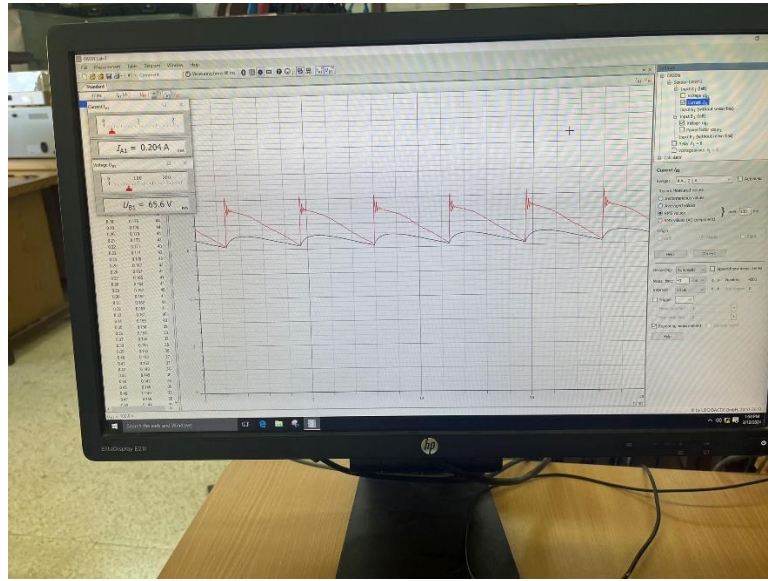


Figure 57: The RMS Voltage of a phase full converter with RL & dealy angle =45

Table 12: The output voltage of a three-phase full-converter with RL & dealy angle =45

	<i>Output voltage</i>	<i>Output Current</i>
RMS values	65.6	0.204
Average Values	59.5	0.192

B. Three-Phase Full-Converter with resistive-inductive Load with dealy angle =90

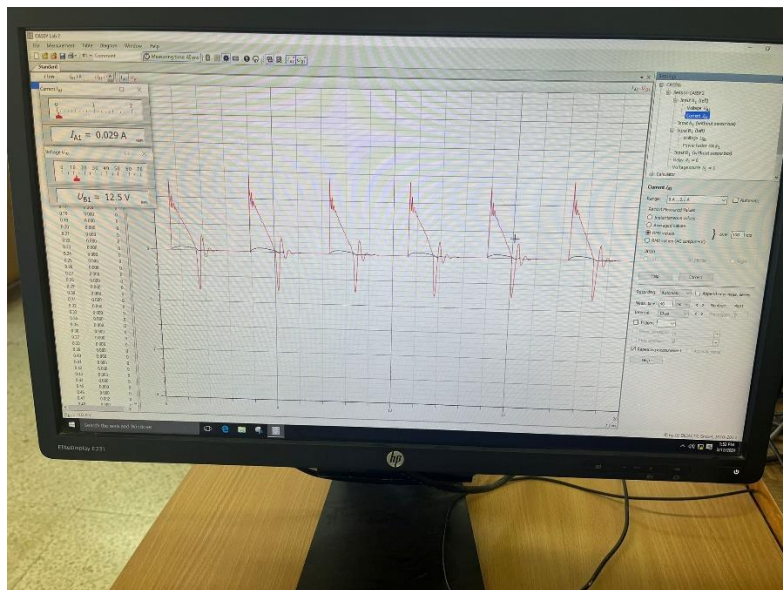


Figure 58: The RMS Output voltage of three-phase converter with RL & dealy angle =90

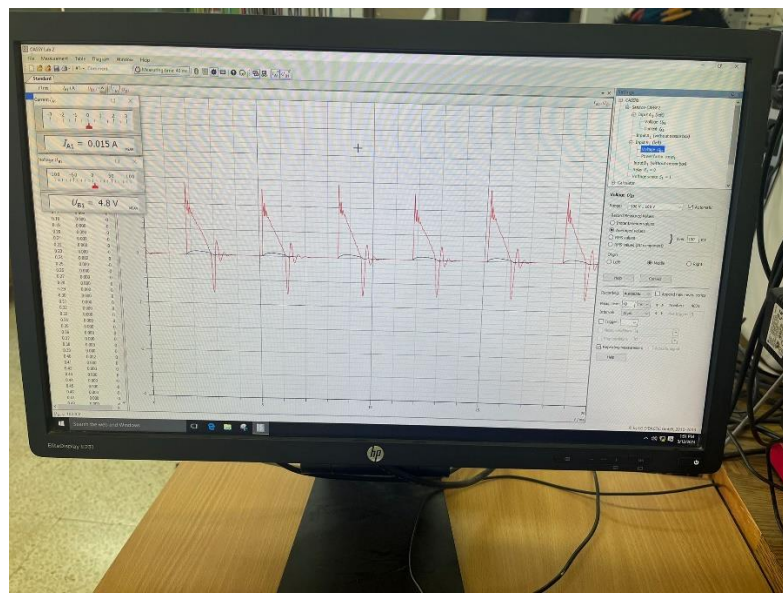


Figure 59: The average output of a three-phase converter with RL & dealy angle =90

Table 12: The Output of a three-phase full converter with RL & delay angle =90

	<i>Output voltage</i>	<i>Output Current</i>
RMS values	12.5	0.029
Average Values	4.8	0.015

When comparing the results obtained for the purely resistive load with those obtained for the RL (resistive-inductive) load at two different delay angles, 45° , and 90° , several differences emerge in terms of the waveforms of the output voltage and current, as well as their average and RMS values. Firstly, at a delay angle of 45° , both the RMS and average values of the output voltage are significantly higher for the RL load compared to the purely resistive load. This difference indicates that the inclusion of inductance in the load results in a higher output voltage. Similarly, the RMS and average values of the output current are also higher for the RL load, suggesting increased current flow through the load due to the presence of inductive elements. Conversely, at a delay angle of 90° , the situation changes. Here, the RMS and average values of the output voltage are considerably lower for the RL load compared to the purely resistive load. This reduction can be attributed to the inductive nature of the load, which tends to oppose changes in current flow, leading to a decrease in voltage. Similarly, the RMS and average values of the output current are also lower for the RL load, indicating reduced current flow through the load compared to the purely resistive case. In terms of waveform characteristics, the output voltage and current waveforms for the RL load exhibit more pronounced fluctuations and delays compared to the purely resistive load, especially at a delay angle of 90° . This behavior is expected due to the presence of inductance in the load, which introduces additional dynamics into the system. Overall, these comparisons highlight the significant influence of load type and delay angle on the behavior and performance of a three-phase full converter. The presence of inductance in the load introduces complexities that impact both the magnitude and dynamics of the output voltage and current waveforms.

5. Discussion and Results

A. Three-Phase Half-wave Converter

The performance of a three-phase half-wave converter is significantly influenced by the type of load connected to it, whether resistive (R), inductive (L), or a combination of both (RL). When considering the resistive load, the converter demonstrates relatively stable performance, as reflected by the calculated form factor (FF) and ripple factor (RF) values. With a resistive load, the output waveform remains relatively smooth, with minimal fluctuations or distortions. In contrast, the introduction of an inductive load introduces additional complexities to the converter's operation. The form factor and ripple factor values for the resistive-inductive (RL) load configuration are notably higher compared to the purely resistive load case. This increase suggests that the output waveform experiences more significant fluctuations and distortions, primarily due to the presence of inductive elements in the load. Additionally, the transformer utilization factor (TUF) tends to decrease when an inductive load is added, indicating a less efficient utilization of the converter's capacity. Moreover, varying the delay angle also influences the converter's performance. At a delay angle of 45° , the output waveform exhibits a slightly higher form factor and ripple factor compared to a delay angle of 90° . This difference suggests that adjusting the delay angle can impact the converter's ability to smooth out fluctuations in the output waveform. In summary, the type of load and the delay angle significantly affect the performance of the three-phase half-wave converter. While a purely resistive load results in relatively stable operation, the introduction of inductive elements leads to increased waveform distortions and reduced efficiency. Additionally, adjusting the delay angle can further impact the converter's ability to regulate the output waveform. These considerations are essential for designing and optimizing the performance of three-phase power conversion systems in various applications.

B. Three-Phase Semi-Converter

When comparing the results obtained with purely resistive (R) loads to those obtained with resistive-inductive (RL) loads for two different delay angles in a three-phase semi-converter, significant differences emerge in terms of output voltage waveforms, as well as their average and RMS values. For the purely resistive load case, at a delay angle of 45° , the output voltage demonstrates higher RMS and average values compared to the RL load. This difference indicates that the resistive-inductive load configuration introduces additional complexities, leading to a reduction in the output voltage levels. Similarly, at a delay angle of 90° , the output voltage exhibits lower RMS and average values for the RL load compared to the purely resistive load case. This discrepancy highlights the impact of inductive elements on the performance of the semi-converter, resulting in reduced output voltage

levels. Moreover, when considering the waveform characteristics, the RL load configuration tends to introduce more pronounced fluctuations and distortions in the output voltage waveform compared to the purely resistive load case. This observation is consistent with the higher ripple factor values calculated for the RL load scenario, indicating a greater degree of waveform irregularity and AC content in the output voltage. In terms of the delay angle, varying the angle from 45° to 90° also influences the output voltage characteristics. Specifically, increasing the delay angle leads to a decrease in both the average and RMS values of the output voltage for both resistive and RL load configurations. This trend suggests that adjusting the delay angle can impact the converter's ability to regulate the output voltage levels, with higher delay angles resulting in lower output voltage magnitudes. In summary, the type of load (purely resistive vs. resistive-inductive) and the delay angle significantly affect the performance of the three-phase semi-converter. The presence of inductive elements in the load introduces additional complexities and leads to reduced output voltage levels and increased waveform irregularities. Furthermore, adjusting the delay angle influences the output voltage levels, with higher delay angles resulting in lower output voltage magnitudes for both resistive and RL load configurations. These findings underscore the importance of considering load characteristics and delay angle settings in the design and optimization of three-phase semi-converters for various applications.

C. Three-Phase Full-Converter

When comparing the results obtained for a purely resistive load to those obtained for an RL (resistive-inductive) load in a three-phase full converter, significant differences emerge in terms of the waveforms of the output voltage and current, as well as their average and RMS values. For the purely resistive load case, at a delay angle of 45° , the output voltage demonstrates higher RMS and average values compared to the RL load. This discrepancy indicates that the introduction of inductive elements in the load leads to a reduction in the output voltage levels and alters the waveform characteristics. Additionally, the ripple factor for the RL load is higher compared to the purely resistive load, indicating a greater degree of waveform irregularity and AC content in the output voltage. Furthermore, at a delay angle of 90° , the differences between the purely resistive and RL load configurations become more pronounced. The RMS and average values of the output voltage for the RL load are significantly lower compared to the purely resistive load case, reflecting the impact of inductive elements on the performance of the full converter. Additionally, the ripple factor for the RL load is considerably higher, indicating a more distorted waveform compared to the purely resistive load. Commenting on the output voltage and current waveforms, it is evident that the presence of inductive elements in the load introduces more pronounced fluctuations and distortions in the output waveform compared to the purely resistive load case. These fluctuations are reflected in higher ripple factor values, signifying a greater degree of waveform irregularity and AC content in the output voltage. In summary, the type of

load (purely resistive vs. resistive-inductive) and the delay angle significantly influence the performance of the three-phase full converter. The introduction of inductive elements in the load leads to reductions in output voltage levels and alterations in waveform characteristics, resulting in more distorted waveforms compared to the purely resistive load case. These findings highlight the importance of considering load characteristics and delay angle settings in the design and optimization of three-phase full converters for various applications.

6. Conclusion

In conclusion, this experiment provided valuable insights into three different topologies of three-phase power converters: the Half-Wave Controlled Rectifier, Semi-Converter, and Full-Converter. Through practical experimentation and analysis, we learned that the Semi-Converter and Full-Converter yielded the best output values, with the Full-Converter exhibiting the highest frequency output. Additionally, we observed significant differences in output characteristics when introducing resistive and inductive loads, with a notable decrease in RMS values when an inductor was added. Furthermore, the effect of the delay angle on output values was explored, revealing a decrease in output values with an increase in delay angle. Despite minor discrepancies between practical results and theoretical predictions, attributed to measurement inaccuracies, the overall alignment between the two indicates the effectiveness of the experimental approach. This comprehensive experiment, although lengthy, provided a wealth of information crucial for understanding the behavior of three-phase power converters and their performance under various conditions. Additionally, the analysis underscored the limitations of the half-wave converter and emphasized the advantages of semi and full-wave converter topologies, particularly in terms of transformer utilization and output waveform quality. Overall, this experiment serves as a foundational component in the study of power electronics, offering valuable insights for future research and practical applications in the field.

7. References

- [1] [Online]. Available:
] <https://drive.google.com/drive/folders/1OrQoMlIVRkgQoC7Vusmz6mQzRH8AGj4e>. [Accessed 16 3 2024].
- [2] [Online]. Available:
] https://kaliasgoldmedal.yolasite.com/resources/Power_Electronics/THREE%20PHASE%20CONTROLLED%20RECTIFIERS.pdf. [Accessed 19 3 2024].
- [3] [Online]. Available: https://protorit.blogspot.com/2013/02/three-phase-half-wave-controlled-rectifier.html#google_vignette. [Accessed 19 3 2024].
- [4] [Online]. Available: <https://www.eeeguide.com/three-phase-semi-converter-feeding-separately-excited-dc-motor/>. [Accessed 19 3 2024].
- [5] [Online]. Available: <https://www.scribd.com/doc/170348499/3-Phase-Semi-Converter-With-Source-Inductance-Ppt>. [Accessed 19 3 2024].
- [6] [Online]. Available: <https://www.electronics-tutorials.ws/power/three-phase-rectification.html>. [Accessed 19 3 2024].
- [7] [Online]. Available: <https://eng-old.najah.edu/ar/node/1480>. [Accessed 19 3 2024].
]
- [8] [Online]. Available: <https://www.sciencedirect.com/topics/engineering/three-phase-rectifier>. [Accessed 19 3 2024].